ARTICLE IN PRESS

Predictive Modeling and Experimental Validation of Mechanical–Microstructural Relationships in 3D-Printed Onyx–Fibre Composites

Bhagyashri Hiralal Dhage[1], Nitin K. Khedkar[2], Mithul J. Naidu[3], Sachin Salunkhe[4*], Lenka Cepova[5], Emad Abouel Nasr[6]

[1]PhD Scholar, Department of Mechanical Engineering, Symbiosis Institute of Technology, Symbiosis International (Deemed University), Pune, India – 412115.

Email: bhagyashri.dhage.phd2023@sitpune.edu.in

[2]PhD guide, Symbiosis International University, and Professor at MIT World Peace University, Pune, India- 411038

Email: nkkhedkar@gmail.com

[3]Faculty of Mechanical Engineering, Tolani Maritime Institute, Pune, India- 410507

[4a]Department of Biosciences, Saveetha School of Engineering, Saveetha Institute of Medical and Technical Sciences, Chennai, India

[4b]Gazi University Faculty of Engineering, Department of Mechanical Engineering, Maltepe, Ankara, Turkey

[5]Department of Machining, Assembly and Engineering Metrology, Faculty of Mechanical Engineering, VSB—Technical University of Ostrava, 70800 Ostrava, Czech Republic

[6]Department of Industrial Engineering, College of Engineering, King Saud University, P.O. Box 800, Riyadh 11421, Saudi Arabia

*Corresponding author Email: sachinsalunkhe@gazi.edu.tr

ARTICLE IN PRESS

ABSTRACT

Additive Manufacturing (AM) has emerged as a revolutionary fabrication technology for producing high-performance polymer-based composite materials. Fused Filament Fabrication (FFF), a leading AM technology, facilitates the fabrication of continuous fibres in a thermoplastic matrix to provide a customised mechanical response. In this study, the tensile and flexural properties of Onyx matrix composites reinforced with continuous carbon fibre (CF) and glass fibre (GF) are investigated. Specimens were fabricated using a Markforged 3D printer and tested in accordance with ASTM standards. A Taguchi L27 design was employed to examine the effect of infill density, fibre volume fraction, fibre orientation, and roof and floor layers. The principal results indicated maximum tensile strengths of 286.8 MPa (CF) and

ARTICLE IN PRESS

183.2 MPa (GF), and a flexural strength of 208.4 MPa (CF). ANOVA indicated the significance of the variables (high F-values, low residuals), especially in the CF flexural and GF tensile models. The regression analysis provided high predictive accuracy for all models, with predicted R-squared values of 98.73% (CF flexural), 97.69% (GF tensile), 91.04% (GF flexural), and 84.22% (CF tensile). Separate machine learning models trained on experimental data further predicted mechanical properties: a linear regression model provided R^2=99.49% for flexural data, while a multi-output random forest model predicted tensile strength and elongation with R^2=99.38% and 96.95%, respectively. SEM analysis of the fractured specimens validated failure modes, such as fibre pullout, matrix cracking, and delamination in CF (brittle) compared to ductile debonding in GF. The integrated Taguchi-ANOVA, machine learning, and microstructural analysis offers a robust platform for optimising the performance of FFF-fabricated fibre-reinforced Onyx composites.

Keywords: *Machine learning, multi-output prediction, Regression Analysis, Taguchi design, Additive Manufacturing, Onyx matrix composites, Carbon fibre, Glass fibre, SEM Analysis, etc.*

Abbreviation	Full Form
3D	Three-Dimensional
AM	Additive Manufacturing
CF	Carbon Fibre
GF	Glass Fibre
FFF	Fused Filament Fabrication
DOE	Design of Experiments
ANOVA	Analysis of Variance
ML	Machine Learning
R^2	Coefficient of Determination
SVR	Support Vector Regression
MSE	Mean Squared Error
SEM	Scanning Electron Microscopy
MPa	Megapascal
RF	Random Forest
VIF	Variance Inflation Factor
NSGA-II	Non-dominated Sorting Genetic Algorithm II
RBF	Radial Basis Function

ARTICLE IN PRESS

1. Introduction

Additive Manufacturing (AM), also known as 3D printing, has recently been recognized as a revolutionary manufacturing technology that allows for the layer-wise fabrication of complex three-dimensional parts directly from digital designs. Compared with traditional subtractive manufacturing, AM provides enhanced design flexibility, minimized material waste, and fast development from design to functional prototyping [1–10]. Among the various AM technologies, Fused Filament Fabrication (FFF) is one of the most popular and widely used methods owing to its low cost, ease of operation, and ability to create complex geometries with acceptable mechanical properties [11,12].

ARTICLE IN PRESS

Composites are a class of engineered materials that consist of two or more different phases, which work together in a synergistic manner to achieve outstanding properties that are not attainable by individual components. Fibre-reinforced polymer composites have been of great interest for use in applications requiring high strength-to-weight ratios, such as in the aerospace, automotive, transportation, and sports industries [13–15]. In the context of AM, the development of fibre-reinforced thermoplastic composites has enabled the rapid creation of lightweight structural components with improved mechanical properties. While short-fibre reinforcement offers moderate enhancements in stiffness and strength, continuous fibre reinforcement offers significantly higher load-carrying capabilities, better anisotropy management, and improved structural efficiency [16–19].

Recent developments in FFF have made it possible to print continuous fibres in thermoplastic matrices, and this has led to significant improvements in mechanical properties. Continuous Filament Fabrication (CFF), used in commercial printers such as Markforged, uses a dual-nozzle system to print both the polymer matrix and continuous fibres, such as carbon and glass fibres [17,20–27]. Among the various types of matrices used, Onyx, a nylon-based filament reinforced with chopped carbon fibres, has gained popularity for its high strength, toughness, dimensional stability, and chemical resistance. Studies have shown that Onyx has significantly higher stiffness and strength than conventional thermoplastics such as ABS, making it a good matrix for continuous fibre-reinforced composite materials [28–33].

The mechanical properties of fibre-reinforced composites printed using FFF are very much dependent on processing conditions. Factors such as fibre orientation, fibre volume fraction, infill density, infill pattern, and roof and floor layers have been found to significantly affect load transfer, interlayer bonding, and failure modes [11,23,34–38]. Therefore, optimising these processing variables is necessary to achieve application-specific mechanical properties. Table 1 presents representative studies from the literature, highlighting process parameters, filament materials, output responses, experimental techniques, and optimisation methods.

Table 1. Summary of Process Parameters and Mechanical Properties in 3D Printing

Author (Year) & Title	**Input Process Parameters**	**Filament Material**	**Method/Technique**	**Key Mechanical Outputs**
Faidallah et al. (2025)	Build orientation, fibre content (10% CF), layer height, printing temperature	CF-reinforced PLA, PETG	FDM; tensile & compression tests	Tensile and compressive strength, young modulus; PLA outperformed CFPLA and

ARTICLE IN PRESS

				PETG by 30-100%
Abualbandora (2025)	Fibre volume fraction, printing speed, nozzle temperature, infill density	Short carbon fibre reinforced composites	Review of FDM parameter effects	Printing parameters highly influence tensile, flexural, and compressive strength.
SezemskÃ½ et al. (2025).	Fibre surface treatment, fibre loading, printing parameters	Onyx + fibreglass layers	Additive manufacturing, mechanical testing	Flexural strength & stiffness enhanced; fibre layers critical for mechanical improvement
Wang et al. (2025)	Infill density, print orientation, fibre content, deposition pattern	Glass fibre/PLA, Carbon fibre/PLA composites	DIC and mechanical testing	Tensile strength, stiffness, impact resistance increased; 20 wt% GF doubled tensile strength; infill & orientation vital
Ismail et al. (2025)	Fibre content (1-5 wt%), extrusion method	GF/PLA	3D printing, tensile testing	Tensile strength peaks at ~2.4% fibre content, drops at 5%
Begum et al. (2025)	Printing orientation (0°, 45°, 90°), fill density (40-60%)	GF/PLA	FDM flexural testing	Max flexural strength ~25 MPa at 90° orientation, 60% fill density
Kaptan & Kartal (2024)	Layer thickness, print speed, nozzle temperature, infill pattern	Continuous carbon fibre prepreg filament	Modified FDM w/ continuous fibre printing	Significant flexural strength & modulus gains; layer thickness key factor
KÃ¡mÃ¡n et al. (2024)	Nozzle temperature, layer height, infill pattern, fibre content	Chopped GF-filled nylon	Extrusion-based 3D printing, mechanical tests	Tensile and flexural strengths are sensitive to process parameters
Xie et al. (2024)	Layer thickness, nozzle temperature, printing speed	Continuous CF/PLA hybrid composites	FDM; orthogonal tests, process optimisation	Tensile ~53 MPa, bending ~277 MPa, ILSS ~39 MPa
Jiahui Li et al. (2024) Strain rate dependence in	Layer thickness 0.1-0.125 mm, fibre vol% 21-42%, strain rates 3.3—10µ to 100/s	Onyx + continuous CF, GF,	Markforged Mark Two: tensile testing with video and high-speed recording	UTS increases: CF 21x, GF 17x, Kevlar 15x neat Onyx;

ARTICLE IN PRESS

continuous fibre reinforced composites		Kevlar filaments		strain-rate sensitivity; varied failure modes
Basim El Essawi et al. (2024) Optimisation of fibre angles and infill	Layer height 0.125 mm, infill 30-80%, raster 0°,90°, ±45°, fibre layer position varied	Onyx + continuous carbon fibre	FFF; Markforged X7; tensile tests	Fibre angle has a significant effect on UTS & modulus; infill density is second; layer position affects toughness; strain rate has the least effect
Moreno-NÃºÃ±ez et al. (2024) Impact absorption of Onyx/aramid composites	Gyroid infill, build orientation flat/on-edge, raster 0°/45°	Onyx + aramid fibre (~56% Vf)	Mark Two; Izod impact test (ASTM D4812), statistical analysis	Flat build impact strength Onyx; on-edge raster orientation minimal effect
Sangaletti et al. (2024) Stacking & raster angle on fracture toughness	150 mm beams; stacking horizontal/vertical; raster 0°/90°, +45°/-45°; 100% infill	Onyx	FDM; SENB fracture tests; FEM (Abaqus)	Vertical stacking + 45°/-45° raster raised fracture toughness to 35 N/mm (2.9x horizontal)
Yun JH et al. (2024) 3D-printed Onyx-fibreglass composites	Nozzle 275°C; print speed 100 mm/s; 0-4 fibreglass layers; aligned fibres; 100% infill	Onyx (nylon + 20% short CF) + fibreglass	FDM; tensile & flexural testing (ISO standards); microscopy	Tensile strength increased ~25 MPa per layer; max 146 MPa; flexural modulus up to 42.5 GPa
Vellaisamy & Munusamy (2024) 3D printed carbon fibre sandwich structures	Nozzle 272°C; 0.125 mm layers; fibre orientation 0°, ±45°, 90°; varied core thickness and cell size	Ultra-strong continuous CF + ONYX-FR	Markforged X7; ASTM C364 & C365 compression tests	Highest energy absorption: 132-147 J (up to ~96% better than Al-CFRP); buckling failure mode
Feng P et al. (2024) FRP reinforced cementitious 3D elements	1-2 FRP layers; wrapping/insertion; variable load rates	Cementitious material + GFRP sheets	Compression and 4-point flexural tests; FEA simulation	Columns: peak load up >1400%, deformation >800%; beams: load up 600%, deflection >200%; failure transitioned brittleâ†'ductile
Anh NT et al. (2024) Topology optimisation for additive manufacturing	FDM: 180°C print temp; 0.2 mm layer; topology optimized under 100 N load	ABS plastic	SolidWorks FEA simulation; FDM printing	Weight reduced 43-77% with intact structural integrity; max stress low; safe

ARTICLE IN PRESS

				displacement and strain.
Kantaros & Soulis (2023)	Layer height, infill density, nozzle temperature, print speed	CF/PLA	FFF/FDM printing; mechanical testing	Improved flexural strength and modulus with optimised parameters
Cuchor et al. (2023) Fibre orientation and mechanical properties of Onyx composites	Layer thickness 0.1-0.2 mm; layering parallel/perpendicular to load	Onyx (nylon + chopped CF)	ASTM D638 static tensile test; SEM	UTS is highest (56.14 MPa) with layers parallel to the load; perpendicular, lower (~38-44 MPa)
Lee et al. (2023) Effect of fibre reinforcement on Onyx composites	30% infill; 1-4 CF/GF reinforcement layers; varied positions	Onyx + continuous CF/GF	Markforged Mark Two; ISO 527-4 tensile test	Tensile strength increases with layers; CF strength increases up to ~198%; GF up to ~119%; CF reduces displacement, GF increases it
Moreno-NÃºÃ±ez et al. (2023) Kevlar fibre rings in Onyx composites	Fibre vol% 17-19%; concentric rings (2 or 4)	Onyx + Kevlar rings	ASTM D3039 tensile, ASTM D790 flexural tests	Tensile modulus +400% (9.6 GPa); flexural +140% (4.1 GPa); weak fibre-matrix bonding observed
Eren et al. (2023) Compressive properties with CF, Kevlar, and GF reinforcements	96 layers; fibre vol% 6.25-25%; fibre orientation & distribution varied	Onyx, Nylon + CF, GF, Kevlar	ASTM D695 compression; DIC; SEM	Fibres parallel to load compressive modulus 11%; GF > CF/Kevlar in compression; optimal CF vol% ~12.5%

Despite the growing body of literature on mechanical characterisation, recent studies highlight the need for fracture and failure analysis to achieve a complete understanding of the performance of additively manufactured composites. Studies on the failure of 3D-printed carbon fibre-reinforced polymers have shown that printing-induced defects such as voids, layer gaps, and fibre/matrix debonding can lead to detectable reductions in strength and stiffness [39,40]. Micromechanics-based fracture models also suggest that the initiation and propagation of cracks

ARTICLE IN PRESS

in composite materials are dominated by fibre/matrix interactions and matrix cracking mechanisms, thus forming a theoretical foundation for understanding experimental fracture performance [41]. However, these fracture studies are rarely coupled with process parameter optimisation and predictive models, especially for Onyx-based continuous fibre composites.

Parallel to this, there has been a growing trend towards the use of data-driven modelling techniques to overcome the limitations of experimental-statistical modelling in dealing with the complex nonlinear interactions of multiple process variables. While traditional experimental-statistical modelling methods remain useful, they are limited in scalability and adaptability for high-dimensional design spaces. Machine learning (ML) methods have shown great promise in dealing with nonlinear input-output mappings and multi-output prediction of mechanical properties in additively manufactured composites [42–46]. Regression-based and ensemble ML models, such as interactive linear regression and multi-output random forest models, have been shown to have advantages in terms of predictive accuracy, computational efficiency, cost-effectiveness, and material savings [47–53]

However, there remain great challenges for high-performance applications such as structural components for unmanned aerial vehicles (UAVs) and microturbine blades, where reliable anisotropic strength, weight efficiency, and predictable failure behaviour under complex loading conditions are of prime importance. In particular, there is a lack of material-specific, experimentally validated predictive models for Onyx-based continuous fibre composites optimized for FFF processes, particularly those that can make simultaneous predictions of multiple mechanical properties [54–57].

ARTICLE IN PRESS

The first objective of the current research work is to experimentally assess the influence of important process variables, namely infill density, fibre volume fraction, fibre orientation, and the number of roof and floor layers, on the tensile and flexural properties of carbon and glass fibre-reinforced Onyx composites produced by FFF, following ASTM standards for testing and analysis. The second objective of this research work is to develop and validate machine learning models for predicting tensile strength, elongation, and flexural strength of the composites using these variables. To this end, a Taguchi L27 orthogonal array is utilised to efficiently explore the design space, and scanning electron microscopy of fractured specimens is conducted to analyse the underlying failure mechanisms. This comprehensive experimental-computational approach enhances understanding of structure-property relationships and facilitates data-driven optimisation of lightweight, high-performance FFF composite parts.

2. Materials and methods

2.1. Materials

ARTICLE IN PRESS

Onyx, a proprietary material of Markforged, is characterised by a chopped carbon fibre-reinforced nylon-based material matrix [58–64]. Unlike traditional engineering-grade thermoplastics such as ABS and PLA, it exhibits better stiffness, tensile strength, and dimensional stability [28,35]. Onyx can be used in a wide variety of applications due to its improved abrasion resistance and thermal stability up to 145°C. The matte, smooth surface usually eliminates the need for post-processing [5,9,63,65,66]. Continuous carbon fibre and high-tensile glass fibre have been incorporated as reinforcing elements into the Onyx matrix [17,24,59,64,65,67–70]. Carbon fibre, with its excellent strength-to-weight ratio, offers superior mechanical properties compared to glass fibre [14,20,24,71]. It is resistant to heat, deformation, and impact and is thus suitable for harsh applications [9]. Although glass fibre is not as strong as carbon fibre, it offers a cost-effective solution that still provides suitable heat insulation, durability, and impact strength [12]. Both fibres were introduced into the composite samples for further evaluation and analysis of the material's properties, as listed in Table 2.

Table 2. Mechanical Properties of Onyx [72–74]

Composite Base	**Onyx**	**Carbon Fibre (CF)**	**Glass Fibre (GF**
Tensile Modulus [GPa]	2.4	800	590
Tensile Strain at Break [%]	25	60	21
Flexural Strength [MPa]	71	540	200
Flexural Modulus [GPa]	3	51	22
Density [g/cm3]	1.2	105	105

ARTICLE IN PRESS

2.2. Methods

The Taguchi L27 orthogonal array was chosen to effectively explore the joint behaviour of several FFF process variables, thereby significantly reducing experimental cost compared to a full factorial design [75,76]. This allows for the systematic assessment of infill density, fibre volume fraction, fibre orientation, and roof/floor layers within reasonable limits of material consumption, machine time, and specimen preparation [77]. Machine learning models were utilised to identify nonlinear relationships between process variables and mechanical responses that cannot be comprehensively represented by standard regression analysis [33]. Scanning electron microscopy was employed to link macroscopic mechanical properties with microstructural failure mechanisms, thereby providing physical insight into the data-driven predictions [78–81].

2.2.1. Specimen Preparation

ARTICLE IN PRESS

Optimisation of mechanical properties of fibre-reinforced Onyx-based composites using Mark-Two 3D printer via Taguchi methods and experimental design. The critical parameters for impact resistance are the infill pattern, density, fibre orientation, and number of layers. Triangular patterns enhance stability and stress distribution within the structure; rectangular patterns balance strength with print speed; and gyroid patterns offer isotropic strength and weight reduction, which is vital for efficiency-critical applications [19,37,82,83]. Infill densities of 30%, 45%, and 52% were tested; lower densities reduce weight but may weaken structures, while higher densities improve strength for demanding applications [44,71]. Layer numbers [19,61,84] affect surface integrity and durability, enhancing delamination resistance [71,85]. Kevlar fibre orientations at 0°, 45°, and 90° impact strength: 0° maximizes tensile strength, 45° improves multi-directional toughness, and 90° enhances shear resistance [84,86,87]. Varying fibre volume ensures optimal stiffness and strength, with higher content improving mechanical properties [88]. Using the Design of Experiments (DOE) approach and the Taguchi method, the parameters fibre type, orientation, infill density, infill pattern, and number of layers were systematically optimised, enabling efficient exploration of parameter effects with minimal experimentation [84].

2.2.2. Printing Samples using Markforged Mark-Two 3D Printer

The Mark-Two 3D printer, first introduced by Markforged in 2016, was used to produce composite specimens [19,82]. The small machine combines both Fused Filament Fabrication (FFF) and Continuous Filament Fabrication (CFF) processes to produce reinforced composites with a thermoplastic Onyx matrix and continuous carbon and glass fibres. The printer has a maximum build volume of 320 mm × 132 mm × 154 mm in the x, y, and z directions, respectively. The machine features a dual-nozzle system, with one nozzle dedicated solely to extruding the Onyx matrix, while the other nozzle deposits continuous fibres. Preheating of the filament to the glass transition temperature is performed before extrusion during printing, where the printer head displaces the XY plane during material deposition. Incremental continuous fibres are infused, with termination at each end of a layer, with evidence of the typical layer thickness of 0.125 mm for carbon fibre and 0.1 mm for glass fibre. The Mark-Two does not require a heated build plate, allowing parts to be removed immediately after printing. Fixed Printing Parameters using the Mark-Two Printer given in Table 3. The mechanical characterisation was performed using tensile and flexural tests in accordance with ASTM D638 and ASTM D790 standards, respectively. The geometry of the Specimen was designed in AutoCAD, while slicing was performed using Markforged's in-house Eiger software [20,31,88–90].

Figure 1 (a) depicts the tensile test specimen geometry according to ASTM D638, and Figure 1 (b) illustrates the flexural test specimen according to ASTM D790 standards[92]. The printed test specimens, made of Onyx reinforced with carbon and glass

ARTICLE IN PRESS

fibres via Fused Filament Fabrication, were tested under controlled conditions. The mechanical performance results were further verified using scanning electron microscopy to analyse fracture morphology and fibre–matrix interfacial behaviour.

Table 3. Fixed Printing Parameters using the Mark-Two Printer [14,84,91]

Parameter	Value
Nozzle diameter	0.4 mm
Raster width	0.4 mm
Raster angle	45°
Onyx layer thickness	0.1 mm
Shell thickness	0.8 mm
Build orientation	Flat
Nozzle temperature (Onyx)	270-275 °C
Nozzle temperature (fibre)	250-255 °C
Print speed (Onyx)	Automatic
Print speed (fibre)	Automatic
Fibre layer thickness	0.125 mm (CF), 0.1 mm (GF)



ARTICLE IN PRESS

Figure 1. Tensile and Flexural Test Specimens of Onyx-Based CF and GF Composites
(a) Tensile test specimen geometry as per ASTM D638; (b) Flexural test specimen geometry as per ASTM D790

2.2.3. Experimental Setup

All tensile and flexural tests were conducted on a Tinius Olsen H25KS Universal Testing Machine. The electromechanical machine is equipped with a 25 kN load cell and high-accuracy sensors, enabling precise mechanical characterisation. The machine is operated via specialised software that enables real-time acquisition of force and displacement data. ASTM D638 type specimens were secured under pneumatic grips for tensile testing. A steady crosshead rate uniaxial tensile load was applied along the longitudinal axis until the Specimen fractured. The machine automatically recorded tensile strength and elongation at break. In the flexural test, a three-point bending apparatus was used in accordance with ASTM D790. The specimens were loaded at both ends while force was applied at a constant rate by a middle loading nose, as indicated in Figure 2. This type of setup was used to measure flexural strength and flexural modulus from the force-displacement behaviour. This arrangement enabled consistent, standardised testing of the mechanical properties of Onyx-based CF and GF composites, which was essential for robust statistical and machine-learning analysis in this work.

ARTICLE IN PRESS

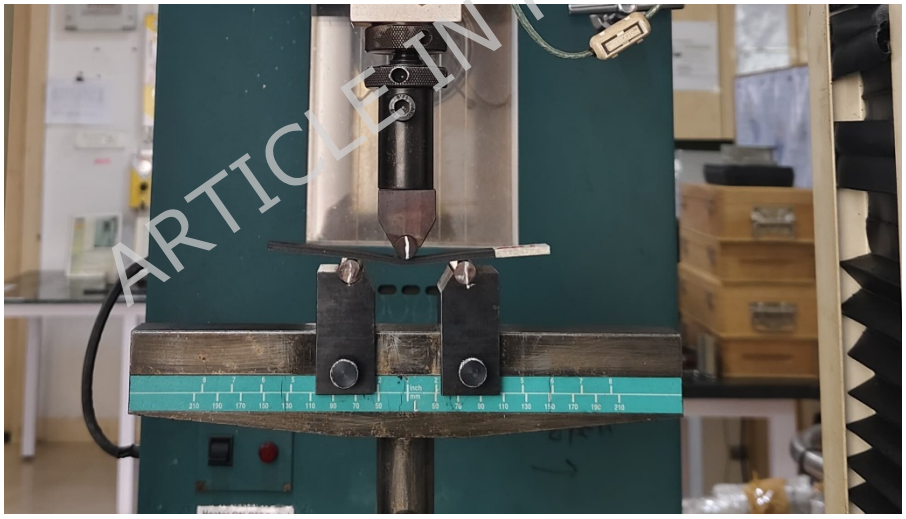

Figure 2. Three-point bending fixture configured according to ASTM D790 standard for testing Onyx-based CF and GF composite specimens

2.2.4. Regression Analysis

Regression analysis was conducted using Minitab 22 to analyse the relationship between key 3D printing process parameters, i.e., fibre volume fraction, infill density, fibre direction, and roof and floor layers, and Onyx-based composite mechanical properties. Separate regression models were developed for tensile and flexural responses, and their validity was verified using statistical measures such as R^2, adjusted R^2,

ARTICLE IN PRESS

predicted R^2, and p-values, which were used to assess the significance and predictive power of each parameter [19,35,86,93].

2.2.5. Training the Machine Learning Algorithm

The experimental results from the Taguchi L27 design were utilised to train supervised machine learning models to learn the nonlinear interactions between the FFF process variables and the resulting mechanical properties. Recent research has shown that integrating learning frameworks with ensemble-based models and statistically structured experimental designs can enhance the predictive accuracy and robustness of machine learning models for additively manufactured composites [40,94].

A multi-output Random Forest Regressor (RFR) was used to model the interdependent mechanical properties of tensile strength and elongation. The performance of the machine learning model was validated using the coefficient of determination (R^2) and mean squared error (MSE). For predicting flexural strength, an interactive linear regression model was used to maintain interpretability while accounting for the interaction effects of the process variables [48–50]. The robustness of the machine learning model was improved by hyperparameter tuning with GridSearchCV, optimising the number of estimators and the maximum tree depth to avoid overfitting while retaining generalisation accuracy. The SHAP analysis was used to evaluate the feature contributions of individual parameters, providing quantitative insight into their relative importance without altering the predictive model [95–97] .

2.2.5. Scanning electron microscopy (SEM)

A microscale study of a fractured composite material reinforced with Onyx-based glass and carbon fibres was carried out using Scanning Electron Microscopy (SEM) to investigate the microstructural features of failure under tensile and flexural loading. Tensile samples exhibited microfeatures, including fibre pullout, longitudinal matrix cracking, and interfacial debonding, indicating poor adhesion and stress-induced axial failure mechanisms. Flexural samples exhibited typical mixed-mode damage, including layer delamination, fibre buckling, and void formation, characteristic of the combined tensile and compressive stresses that develop during bending. The microstructural data provided by SEM well complemented the trends in mechanical performance and helped elucidate the relationship between failure behaviour and process parameters in 3D-printed Onyx-based composites [37,82,98].

3. Results and Discussion

3.1. Mechanical Performance

ARTICLE IN PRESS

Tensile and three-point flexural tests were performed based on ASTM D638 and ASTM D790, respectively (n = 6 for each condition). The mechanical results for all parameter combinations are presented in Table 4.

The combination of carbon fibre-reinforced Onyx with gyroid infill pattern, 30% fibre volume fraction, 0° fibre orientation, and four layers (Set E) showed the best mechanical performance. This combination resulted in a maximum tensile strength of 286.8 MPa and a flexural strength of 206.4 MPa. This is due to efficient stress transfer along the aligned carbon fibres and the continuous stress distribution provided by the gyroid pattern, both of which reduce internal stress concentrations. Conversely, the rectangular infill pattern with a 20% fibre volume fraction and 90° fibre orientation showed the lowest tensile strength of 71.8 MPa, due to inefficient fibre alignment in the loading direction and a discontinuous stress-transfer path within the structure. Visual photographs of the fractured tensile specimens of CF and GF composites are presented in Figures 3 (a) and 3 (b), respectively



Figure 3. Fractured tensile specimens of Onyx-based composites: (a) Carbon fibre (CF); (b) Glass fibre (GF)

Table 4. Mechanical properties of CF and GF reinforced Onyx composites under different processing conditions

Material composition	**Set**	**Infill pattern**	**Infill Density (%)**	**Fibre Volume Fraction (%)**	**Fibre Orientation (°)**	**No of Layers**	**Tensile Strength (MPa)**	**Elongation (%)**	**Flexural Strength (MPa)**
Onyx+CF	A	Triangle	30	40	45	4	155.4 ± 2.11	2.99 ± 0.06	136.9 ± 2.41
	B	Triangle	30	40	45	6	143.0 ± 1.86	3.47 ± 0.06	132.7 ± 2.56
	C	Rectangle	45	20	90	4	71.8 ± 1.05	2.34 ± 0.04	92.5 ± 1.48

ARTICLE IN PRESS

	D	Rectangle	45	20	90	6	87.0 ± 1.71	2.75 ± 0.03	93.9 ± 1.79
	E	Gyroid	52	30	0	4	278.9 ± 5.54	3.48 ± 0.06	203.1 ± 3.45
	F	Gyroid	52	30	0	6	271.7 ± 6.25	3.67 ± 0.07	198.6 ± 3.63
Onyx+GF	A	Triangle	30	20	0	6	180.3 ± 2.77	5.17 ± 0.10	71.3 ± 1.60
	B	Triangle	30	20	0	4	173.8 ± 2.99	4.58 ± 0.09	56.9 ± 1.09
	C	Rectangle	45	30	45	6	131.2 ± 1.96	5.20 ± 0.08	58.6 ± 0.91
	D	Rectangle	45	30	45	4	129.9 ± 2.34	4.91 ± 0.07	60.7 ± 0.95
	E	Gyroid	52	40	90	6	150.5 ± 2.66	5.85 ± 0.08	64.5 ± 0.87
	F	Gyroid	52	40	90	4	144.0 ± 2.44	5.42 ± 0.11	136.9 ± 2.41

The glass fibre-reinforced specimens showed lower tensile strength, with a maximum of 183.2 MPa in their optimal configuration, a reduction of approximately 36% compared to the optimal carbon fibre configuration. The flexural strength of the glass fibre composites reached a maximum of 74.3 MPa, which is significantly lower than the carbon fibre maximum of 208.4 MPa. However, the glass fibre specimens showed higher elongation at break (>4% compared to ~3.5% for carbon fibre), indicating greater ductility. This is because glass fibres are less stiff and exhibit lower fibre-matrix interfacial stiffness, leading to fibre pull-out and energy absorption rather than brittle fracture.

The gyroid infill pattern showed the best tensile and flexural performance for all configurations, while the rectangular pattern showed reduced strength and increased variability. The coefficient of variation across all test sets remained below 2%, indicating high experimental accuracy.

Figure 4(a) presents the tensile stress–strain response of the Onyx+CF composite. The curve exhibits a predominantly linear elastic behaviour up to failure, indicating high stiffness and limited ductility. A maximum tensile strength of 286.8 MPa was achieved with an elongation at break of 3.55%, confirming the rigid and brittle nature of the CF-reinforced composite.

Figure 4(b) shows the tensile stress–strain behaviour of the Onyx+GF composite. Compared to CF, the GF composite demonstrates lower tensile strength (183.2 MPa) but higher elongation at break (5.25%). The curve shows a longer deformation region prior to failure, indicating improved ductility and greater strain-to-failure.

ARTICLE IN PRESS

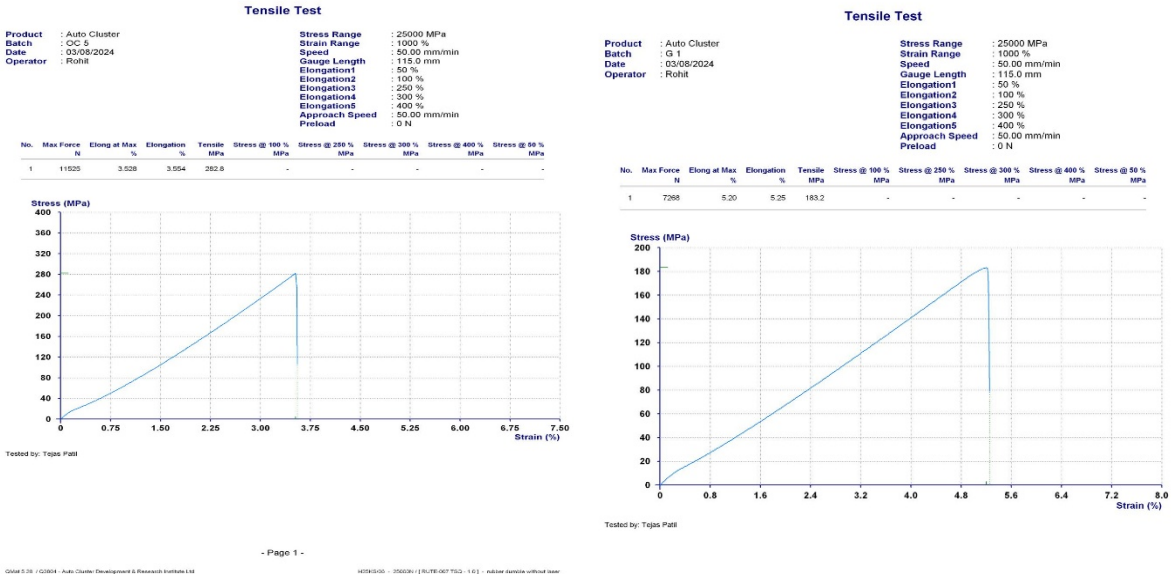

Figure 4 (a–b): (a) Stress–strain diagram of CF-Onyx composite batch showing maximum tensile strength; (b) Stress–strain diagram of GF-Onyx composite showing maximum tensile strength

The flexural force-extension graph for the CF-Onyx composite material is shown in Figure 5(a). The graph shows a steeper linear load deformation, followed by a sudden load drop at failure, which is typical of stiffer and brittle materials. The highest flexural strength recorded is 206.4 MPa, indicating a higher load-carrying capacity under bending.

The flexural force-extension graph for the GF-Onyx composite material is shown in Figure 5(b). Compared to the CF-Onyx specimen, the graph shows a lower slope, indicating a lower stiffness. The highest recorded flexural strength is 74.3 MPa, and the graph also shows a more gradual load drop at failure, indicating higher ductility.

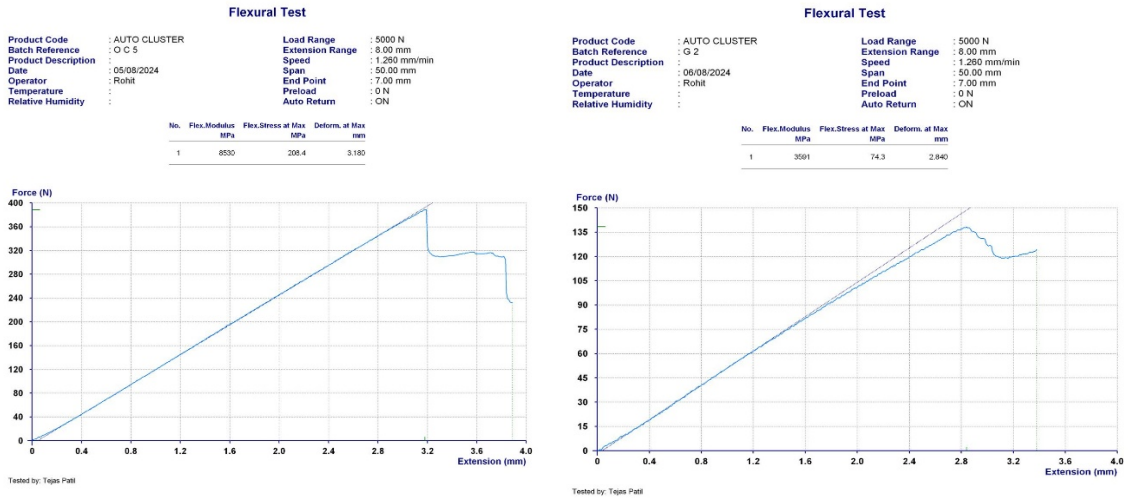

ARTICLE IN PRESS

Figure 5. (a) Force vs. extension diagram of CF-Onyx composite batch showing maximum flexural strength; (b) Force vs. extension diagram of GF-Onyx composite batch showing maximum flexural strength

3.2. Regression Analysis

The results obtained were analysed using Minitab 22 statistical software. Regression analysis was performed for the response variables, Tensile strength (MPa) and Flexural strength, separately, with parameters including material composition, infill density, fibre volume fraction, fibre orientation, and the number of roof and floor layers.

3.2.1. Regression Equation for Tensile Test

The regression equation obtained for tensile strength is given by:

Tensile strength (MPa) = 163.23 + 8.30(Onyx-CF) + 49.65(Gyroid) - 82.85(Rectangular) + 61.32(30% fibre volume fraction) - 0.60(4 layers)

The equation has high predictive ability, with a coefficient of determination (R^2) of 99.44% and a predicted R^2 of 96.75%, indicating a good fit between the experimental and predicted values. The analysis of variance also reveals that the infill pattern and fibre volume fraction are significant factors in determining the tensile strength ($p < 0.001$), as shown in Table 5.

The positive coefficient for the gyroid infill pattern and the higher fibre volume fraction indicate their prominent influence on improving tensile strength, whereas the negative coefficient for the rectangular infill pattern indicates an adverse effect under the current parameter setting.

ARTICLE IN PRESS

Table 5. Regression Coefficients table for tensile test

Term	**Coef**	**SE Coef**	**T-Value**	**P-Value**	**VIF**
Constant	163.23	2.06	79.14	0.000	
Material Composition					
Onyx+CF	8.30	2.06	4.02	0.010	1.00
Infill pattern					
Gyroid	49.65	3.37	14.74	0.000	1.78
Rectangular	-82.85	3.37	-24.60	0.000	1.78
Fibre Volume Fraction%					
20	-7.73	3.37	-2.30	0.070	1.78
30	61.32	3.37	18.20	0.000	1.78

ARTICLE IN PRESS

Number of Roof and Floor Layers					
4	-0.60	2.06	-0.29	0.783	1.00
Model Summary					
	S	**R-sq**	**R-sq(adj)**	**R-sq(pred)**	
	7.14493	**99.44%**	**98.76%**	**96.75%**	

The regression analysis reveals that the statistically significant factors affecting tensile strength are infill morphology and fibre volume fraction. Compared to the triangular reference morphology, the gyroid morphology results in a statistically significant increase in tensile strength of 49.65 MPa ($p < 0.001$), while the rectangular morphology results in a statistically significant reduction of 82.85 MPa ($p < 0.001$). Fibre volume fraction is also a statistically significant factor, and a 30% fibre volume fraction results in a statistically significant increase in tensile strength of 61.32 MPa ($p < 0.001$). However, a 20% fibre volume fraction results in a statistically significant reduction of 7.73 MPa ($p = 0.070$), which is not statistically significant at the 95% confidence level.

The number of roof and floor layers has a negligible effect on tensile properties. A four-layer configuration predicts a 0.60 MPa reduction compared to the six-layer reference configuration ($p = 0.783$), suggesting that variation in surface-layer properties does not significantly affect tensile strength.

3.2.2. Regression Equation for Flexural Test

Flexural Strength (MPa)=105.600 + 40.400 Material Composition Onyx+CF- 40.400 Material Composition Onyx+GF + 24.133 Infill pattern Gyroid-41.267 Infill pattern Rectangular+17.133 Infill pattern Triangular-9.733 Fibre Volume Fraction%20+35.367 Fibre Volume Fraction%30-25.633 Fibre Volume Fraction%40+1.250 No. No. Roof and Floor Layers 4-1.250 No. Of Roof and Floor Layers 6

The regression equation for flexural strength has high predictive capability, with $R^2 = 99.94\%$, adjusted $R^2 = 99.86\%$, and predicted $R^2 = 99.65\%$, presented in Table 6. This indicates that the selected processing variables account for almost all the variability in flexural performance. The intercept is 105.6 MPa. The presence of carbon fibre (Onyx+CF) contributes positively to flexural strength by 40.4 MPa ($p < 0.001$), which can be attributed to the higher stiffness and efficiency of carbon fibres in load transfer during bending.

Table 6. Regression Coefficients table for flexural test

ARTICLE IN PRESS

Term	Coef	SE Coef	T-Value	P-Value	VIF
Constant	105.6	0.575	183.69	0	
Material Composition					
Onyx+CF	40.4	0.575	70.27	0	1
Infill pattern					
Gyroid	24.133	0.939	25.71	0	1.78
Rectangular	-41.267	0.939	-43.96	0	1.78
Fibre Volume Fraction%					
20	-9.733	0.939	-10.37	0	1.78
30	35.367	0.939	37.67	0	1.78
Number of Roof and Floor Layers					
4	1.25	0.575	2.17	0.082	1
Model Summary					
	S	R-sq	R-sq(adj)	R-sq(pred)	
	1.99148	99.94%	99.86%	99.65%	

In the case of infill patterns, the gyroid pattern has a positive effect of 24.13 MPa ($p < 0.001$), while the rectangular pattern has a negative effect of 41.27 MPa ($p < 0.001$) compared to the reference pattern, which indicates the effect of internal geometry on stress and structural continuity. The increase in fibre volume fraction from 10% to 30% has a significant positive effect of 35.37 MPa, confirming the positive effect of higher fibre content on structural strength, whereas a 20% fibre content has a negative effect of 9.73 MPa. The number of roof and floor layers (4 layers) has a marginal, statistically insignificant effect of 1.25 MPa ($p = 0.082$), indicating that the outer layers have a negligible effect compared to the reinforcement's internal geometry. The low standard error ($S = 1.99148$) further confirms the regression model's accuracy and reliability.

3.3. Analysis of Variance (ANOVA)

3.3.1. Analysis of Variance for Tensile Performance

Analysis of results (Table 7) shows that the pattern of infill, fibre volume fraction, and material composition are statistically significant factors that affect the tensile strength. Of these, the pattern of infill has the highest significance ($F = 306.51$, $p < 0.001$), followed by fibre volume fraction ($F = 196.59$, $p < 0.001$). Material composition is still significant ($F = 16.19$, $p = 0.010$). However, the number of roof and floor layers is statistically insignificant ($F = 0.08$, $p = 0.783$). The residual sum of squares is small (SS = 255.3 out of 45,210.5).

Table 7. ANOVA Results for Tensile Strength of Onyx-Based Composites

Source	**DF**	**Adj SS**	**Adj MS**	**F-Value**	**P-Value**

ARTICLE IN PRESS

Material Composition	1	826.7	826.7	16.19	0.010
Infill pattern	2	31294.5	15647.2	306.51	0.000
Fibre Volume Fraction %	2	20072.1	10036.1	196.59	0.000
No. of Roof and Floor Layers	1	4.3	4.3	0.08	0.783
Error	5	255.3	51.1		
Total	11	45210.5			

The trends identified in the main effects plot shown in Figure 6 align with the experimental findings presented in Section 3.1. Carbon fibre reinforcement has a higher mean tensile strength than glass fibre due to its higher modulus and efficient load transfer mechanism in the matrix. The gyroid pattern has the highest tensile strength (~210 MPa), as expected from the optimal configuration identified in Section 3.1, due to its continuous pattern, which ensures efficient stress distribution and avoids stress concentration. In contrast, the rectangular pattern (~110 MPa) induces geometric discontinuities that are less efficient under tensile loading.

The increase in tensile strength with higher fibre volume fraction (52% density) is a result of better interaction between the matrix and fibres, while the intermediate values are less efficient in terms of reinforcement. The orientation of the fibres has a significant effect on tensile strength, with the 0° orientation having the highest strength (~230 MPa), as the fibres are aligned in the direction of the applied load and can withstand the highest amount of stress; other orientations (45° and 90°) are less efficient in terms of load transfer. As expected from both the experimental results and the ANOVA, roof and floor layers have negligible effects, suggesting that tensile failure is less dependent on the thickness of the surface layers.

ARTICLE IN PRESS

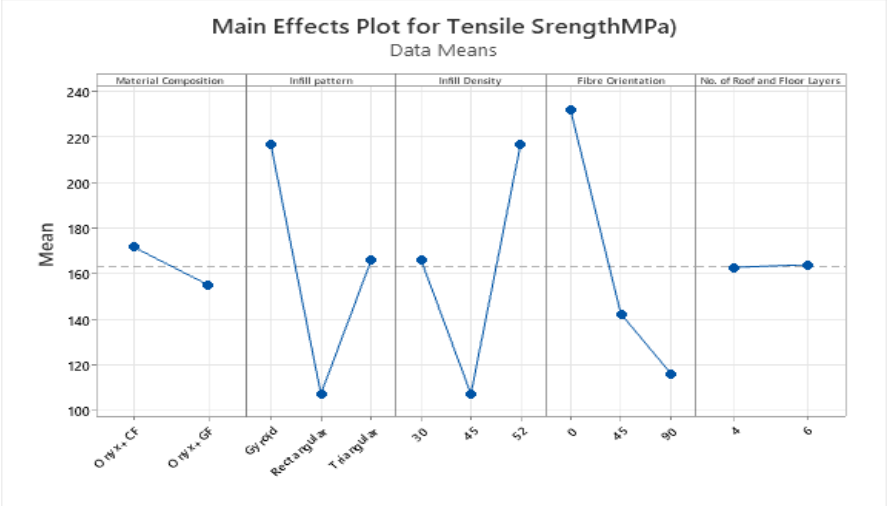

Figure 6. Main Plot for Tensile Strength for Onyx reinforced composite

3.3.1.1. Tensile Strength Analysis through Surface and Contour Plots

ARTICLE IN PRESS

Figure 7 shows contour and surface plots of the interaction effects of significant process parameters on the Onyx fibre composite tensile strength. As seen in Figure 7(a), the concurrent increase in fibre volume fraction and infill density results in a significant increase in tensile strength, with values exceeding 250 MPa observed at higher levels of both parameters. Figure 7(b) shows that low fibre orientation angles (0°–30°), combined with high infill densities, result in enhanced tensile performance, underscoring the importance of aligned fibre directions for load-bearing capacity. Similarly, Figure 7(c) shows that tensile strength increases when low fibre orientation is combined with a high fibre volume fraction, again emphasising the importance of efficient fibre alignment and content. Conversely, Figure 7(d) shows almost no variation in tensile strength across various roof and floor layer combinations with varying fibre volume fractions, corroborating the ANOVA result, which indicated that this factor was statistically insignificant ($p = 0.783$). The 3D surface plot in Figure 7(e) further verifies that tensile strength is highest at areas of high fibre volume and low fibre orientation, reflecting the overriding synergistic effect of these two parameters. Lastly, Figure 7(f) reconfirms that the combination of high infill density and fibre volume fraction yields the best mechanical response, as indicated by the regression and ANOVA results. These plots verify the previous statistical models and emphasise the pivotal role of fibre alignment, infill density, and fibre volume in controlling the tensile performance of Onyx-based fibre composites.

ARTICLE IN PRESS

ARTICLE IN PRESS

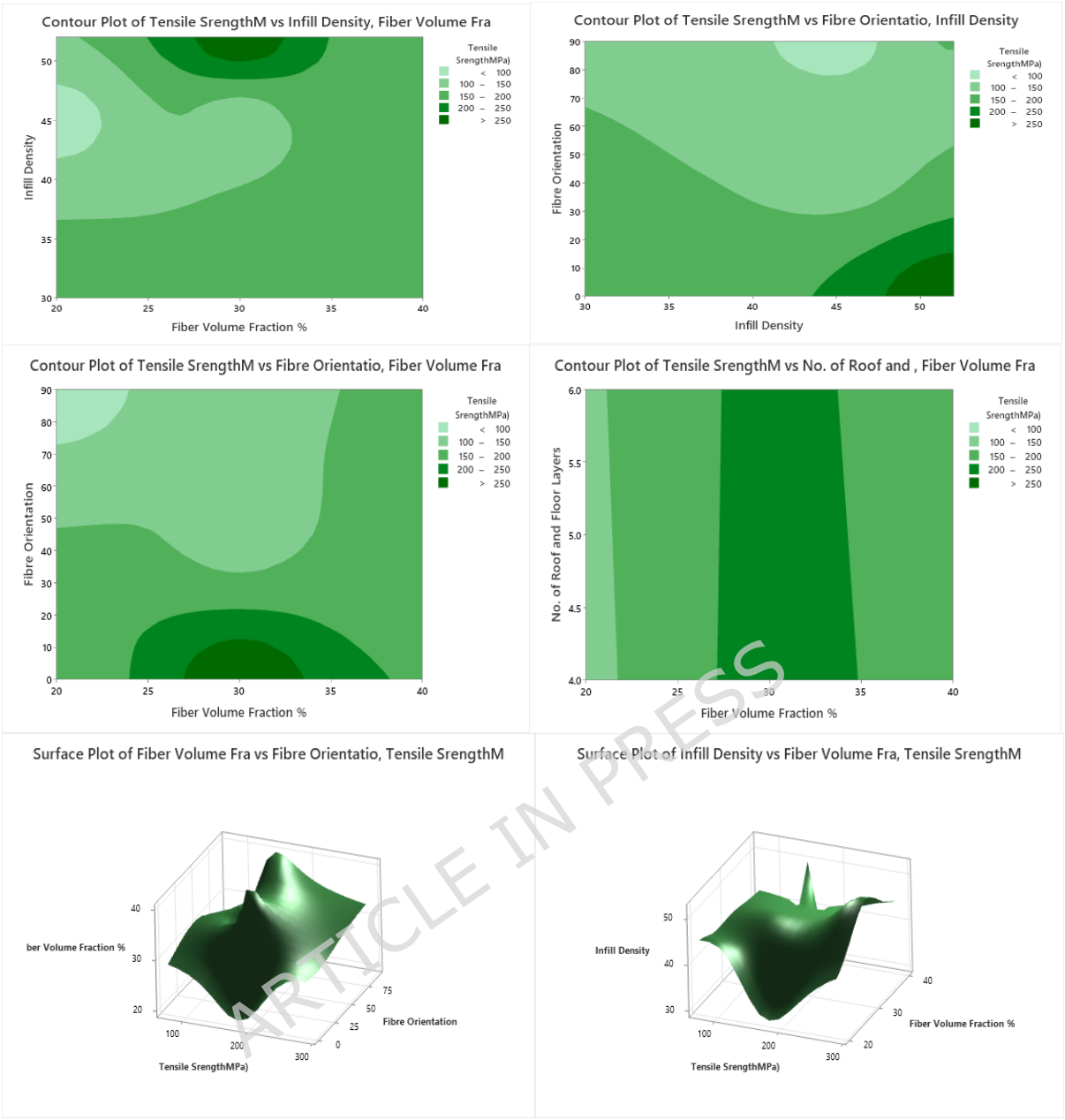

Figure 7. (a) Contour plot of Tensile Strength (MPa) vs. Infill Density and Fibre Volume Fraction; (b) Contour plot of Tensile Strength (MPa) vs. Fibre Orientation and Infill Density; (c) Contour plot of Tensile Strength (MPa) vs. Fibre Orientation and Fibre Volume Fraction; (d) Contour plot of Tensile Strength (MPa) vs. Number of Roof and Floor Layers and Fibre Volume Fraction; (e) Surface plot of Tensile Strength (MPa) vs. Fibre Orientation and Fibre Volume Fraction; (f) Surface plot of Tensile Strength (MPa) vs. Infill Density and Fibre Volume Fraction.

3.3.2. Analysis of Variance for Flexural Performance

ARTICLE IN PRESS

The ANOVA output shown in Table 8, that material composition, infill pattern, and fibre volume fraction are significant variables affecting the flexural strength of Onyx-based composites.

Material composition is the most significant variable ($F = 4938.46$, $p < 0.001$), thus validating that fibre type (CF vs. GF) is the primary factor in determining the bending properties based on the stiffness and load-carrying capacity of the material. The infill pattern is also highly significant ($F = 975.38$, $p < 0.001$), confirming that the material's internal structure directly affects its stress distribution and rigidity during three-point bending tests. Fibre volume fraction is also highly significant ($F = 757.42$, $p < 0.001$), thus validating that the fibre content of the material is a critical factor in determining the resistance to flexural deformation. However, the number of roof and floor layers is not statistically significant ($F = 4.73$, $p = 0.082$), thus confirming that the thickness of the outer shell of the material has a negligible effect compared to the material's internal structure.

The error variance is very low (Adj MS = 4) compared to the treatment effects, thus confirming the adequacy of the model and high signal-to-noise ratio. The analysis thus confirms that material composition is the most significant factor, followed by infill geometry and fibre content, in determining the flexural properties.

Table 8. ANOVA Results for Flexural Strength of Onyx-Based Composites

Source	DF	Adj SS	Adj MS	F-Value	P-Value
Material Composition	1	19585.9	19585.9	4938.46	0
Infill pattern	2	7736.7	3868.4	975.38	0
Fibre Volume Fraction %	2	6007.8	3003.9	757.42	0
No. of Roof and Floor Layers	1	18.8	18.8	4.73	0.082
Error	5	19.8	4		
Total	11	32235.1			

ARTICLE IN PRESS

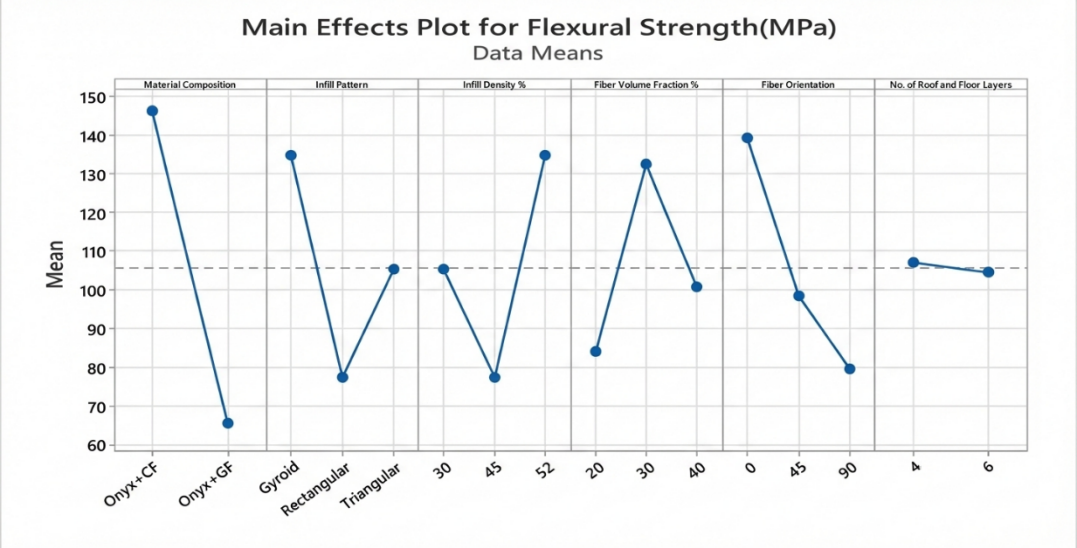

Figure 8. Main Plot for Flexural Strength for Onyx reinforced composite

Figure 8 shows trends consistent with the statistical results and experimental data. The increased mean flexural strength of Onyx+CF (~147 MPa) compared to Onyx+GF (~67 MPa) reflects the enhanced modulus and ability to transfer loads between the carbon fibre and the matrix. The gyroid pattern (~136 MPa) performs better than the triangular and rectangular patterns because of its curvature-based, non-discrete topology, which is beneficial for stress distribution and minimising stress concentrations during bending. Optimal performance at 52% infill density and 30% fibre volume fraction suggests an optimal reinforcement level beyond which defects, voids, and fibre overloading can impair efficiency. The high sensitivity to 0° fibre orientation (~140 MPa) further supports the directional reinforcement concept, which suggests that optimal resistance to crack formation and propagation is achieved by aligning the fibres with the tensile surface of the beam during bending. All the above results are consistent with composite beam theory and support the conclusion that the internal structure and fibre orientation are the dominant factors influencing the flexural properties of additively manufactured Onyx composites.

3.3.2.1. Flexural Strength Analysis through Surface and Contour Plots

The interaction effects of different printing parameters on the flexural strength of Onyx-based fibre composites are graphically illustrated in Figure 9(a–f) using contour and surface plots. Figure 9(a) displays the contour plot of infill density vs. fibre orientation such that maximum flexural strength takes place at higher infill densities (around 50%) and lower fibre orientation angles (0°–30°), which indicates that fibres oriented in the direction of load improve structural stiffness. Figure 9(b), the infill density vs. fibre volume fraction, shows that strength increases with infill density and reaches a maximum at a moderate fibre volume fraction (~30%), indicating that excessive fibre volume leads to defects or poor bonding. Figure 9(c) displays fibre volume fraction vs. number of roof

ARTICLE IN PRESS

and floor layers, where there is minimal variation in flexural strength, indicating that the top/bottom layer number has no appreciable effect on bending performance. Figure 9(d) displays the interaction between fibre volume fraction and fibre orientation, further confirming that flexural strength is maximised when fibres are moderately concentrated and oriented between 0° and 30°, which assures optimal load transfer. The 3D surface plot in Figure 9(e) shows that the maximum flexural strength is achieved with ~50% infill and a fibre volume fraction of around 30%, forming a peak in strength. Figure 9(f) also shows that the optimal pair of fibre volume fraction and low orientation angle yields the maximum flexural strength. The total plots indicate that infill density, fibre volume fraction, and fibre orientation are the most critical parameters. At the same time, the number of roof and floor layers has a minimal contribution to flexural strength.

ARTICLE IN PRESS

ARTICLE IN PRESS

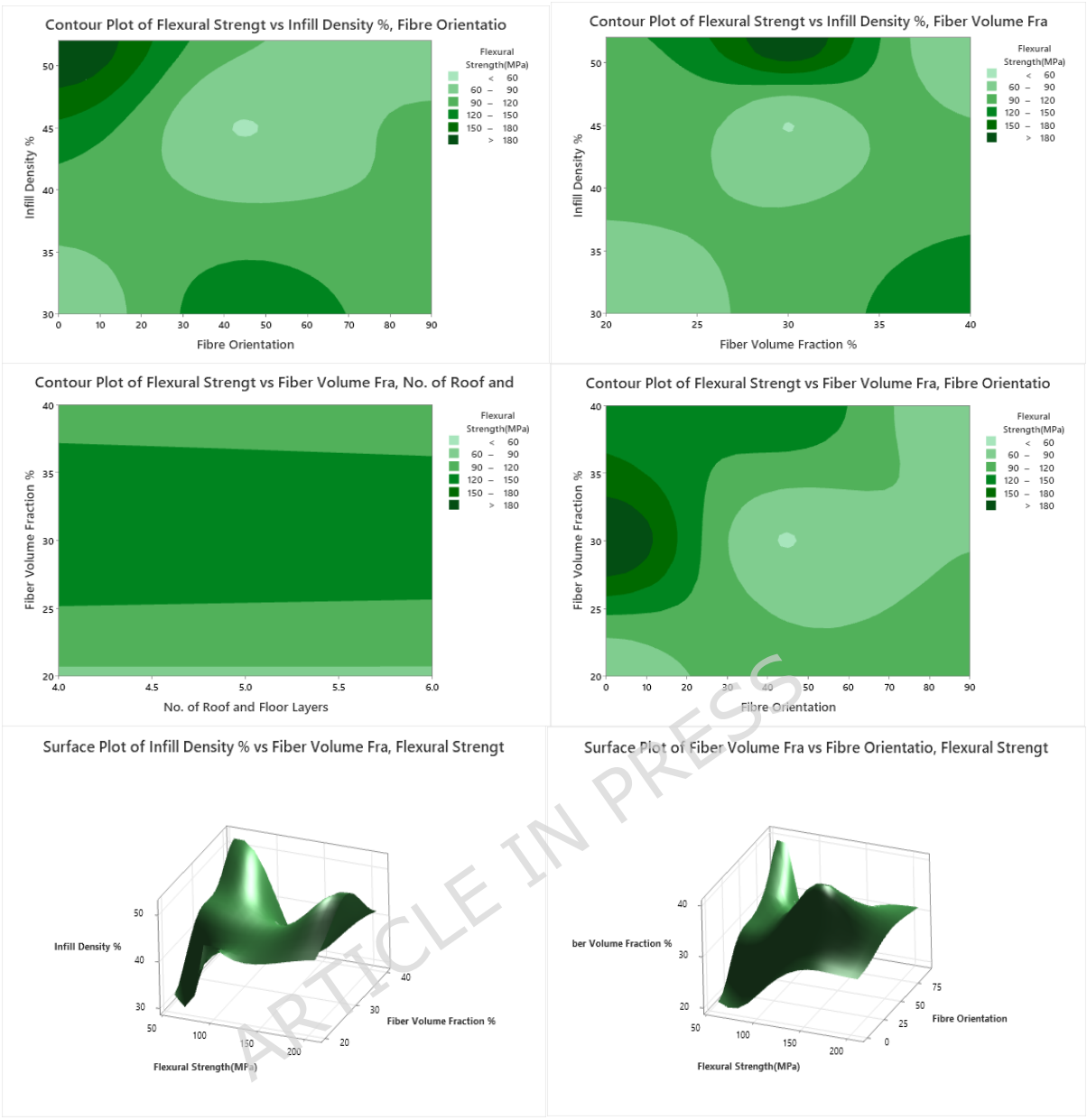

Figure 9**.** (a) Contour plot of Flexural Strength (MPa) vs. Infill Density and Fibre Orientation; (b) Contour plot of Flexural Strength (MPa) vs. Infill Density and Fibre Volume Fraction; (c) Contour plot of Flexural Strength (MPa) vs. Fibre Volume Fraction and Number of Roof and Floor Layers; (d) Contour plot of Flexural Strength (MPa) vs. Fibre Volume Fraction and Fibre Orientation; (e) Surface plot of Flexural Strength (MPa) vs. Infill Density and Fibre Volume Fraction; (f) Surface plot of Flexural Strength (MPa) vs. Fibre Volume Fraction and Fibre Orientation.

3.4. Performance Evaluation of Machine Learning Models for Tensile Strength Prediction

A supervised machine learning approach was proposed to predict tensile strength values in MPa and elongation at break values in percentages of

ARTICLE IN PRESS

Onyx-based 3D-printed fibre composite materials containing carbon and glass fibres. The original dataset consisted of 162 specimens that were experimentally fabricated and mechanically tested according to a Taguchi design of experiments L27 orthogonal array, with six replicates at each parameter configuration. To avoid data leakage and provide a statistically sound evaluation, specimens were first clustered based on their parameter configurations. Subsequently, the original dataset was split at the specimen level using an 80:20 ratio, yielding 126 specimens for training and 36 specimens for testing, with 21 and 6 configurations, respectively.

To provide added robustness to the proposed machine learning approach and enhance the stability of the learning process within the experimentally validated domain, a controlled data augmentation strategy was employed solely on the training dataset. No data augmentation was performed on the testing dataset. Synthetic data were generated using statistically controlled perturbation of the original experimental data points, ensuring that the generated synthetic data points were within the original design space defined by the Taguchi design of experiments. As a result, the training dataset was expanded to 410 samples, while the testing dataset contained 36 purely experimental specimens.

The feature space for the model consisted of six different parameters associated with the manufacturing process, namely material, infill pattern, infill density, fibre volume fraction, fibre orientation, and number of roof/floor layers. Categorical variables such as material composition, infill pattern, and fibre orientation were treated as categorical variables in MATLAB, which internally converts these variables to their corresponding indicator form. To predict the tensile strength as well as elongation at break, the model used a multi-output Random Forest Regressor. This allowed for the possibility of correlation between the two different output parameters. The hyperparameters of the model were optimised using GridSearchCV along with five-fold cross-validation, only for the augmented training set. This ensured that the model did not overfit. The model configuration that gave the best performance had 200 decision trees (n_estimators = 200) with a maximum depth of 20 (max_depth = 20). The model had an R^2 value of 0.946 along with an MSE of 54.23 MPa^2 for predicting the tensile strength. For predicting elongation, the model had an R^2 value of 0.913 along with an MSE of 0.0921. These are strong predictions for the range of parameters considered in the experimental setup.

3.4.1. Correlation Analysis

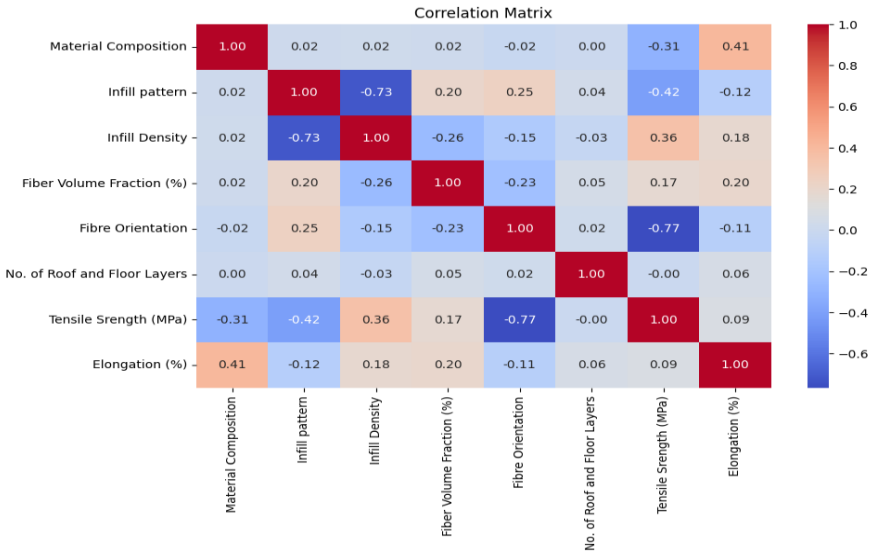

Figure 10. Pearson Correlation Heatmap of Input Features and Tensile Strength in Onyx-Fibre Composites

Figure 10 illustrates the correlation matrix, which depicts the interdependencies among the key input parameters and target outputs, specifically tensile strength and elongation. Surprisingly, fibre orientation is strongly negatively correlated with tensile strength ($r = -0.77$), indicating that an increase in the deviation of the fibre angle from the direction of loading is associated with a significant reduction in tensile strength. This concurs with the experimental results and ANOVA results, which indicate that fibre orientation is an important parameter. Similarly, the infill pattern is moderately negatively correlated with tensile strength ($r = -0.42$), concurring with the regression model results, which reported high statistical significance ($F = 306.5$). Fibre volume fraction and infill density exhibit low positive correlations with tensile strength ($r = 0.17$ and 0.36, respectively), indicating their positive effect on mechanical strength. Surprisingly, the roof and floor layers are nearly uncorrelated with the outputs, consistent with their negligible contribution, a finding supported by both statistical tests (ANOVA, $p > 0.05$) and machine-learning-based feature importance scores. Additionally, the positive correlation between material composition and elongation ($r = 0.41$) suggests that shifting from carbon fibre to glass fibre tends to increase overall ductility, consistent with both experimental results and machine learning predictions. Generally, the pattern of correlation confirmed the reliability and reproducibility of results from both statistical modelling and machine learning approaches, thereby validating the synergistic approach adopted in this study.

ARTICLE IN PRESS

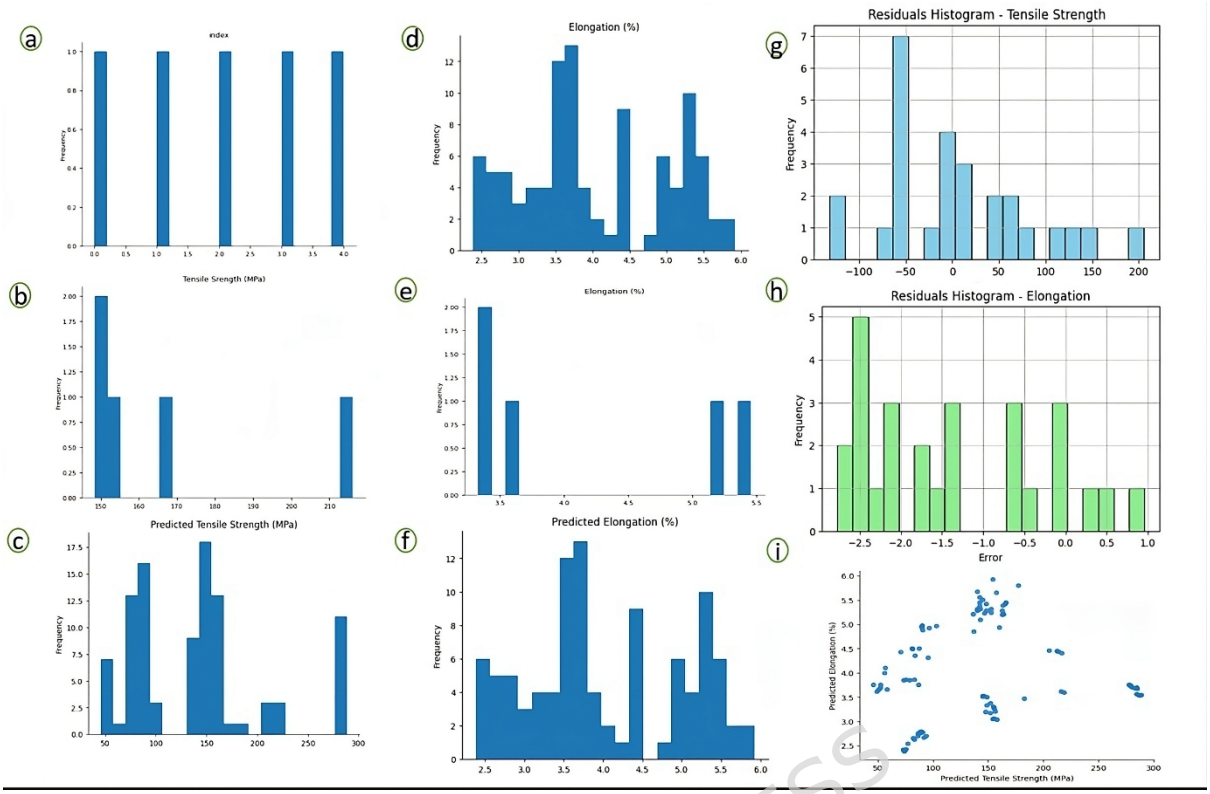

Figure 11. (a) Bar chart of sample indices, (b) Histogram of experimental tensile strength, (c) Histogram of predicted tensile strength, (d) Histogram of experimental elongation, (e) Histogram of predicted elongation, (f) Full predicted elongation histogram, (g) Residual histogram of tensile strength, (h) Residual histogram of elongation, (i) Scatter plot of predicted tensile strength vs. elongation.

Figure 11 illustrates the distribution, prediction, and residual analysis of the fibre-reinforced tensile strength and elongation of Onyx composites using machine learning modelling. The x-axis is used for the sample index, and the y-axis for frequency, in Figure 11(a). The bar graph shows the number of samples used to analyse and ensure data input consistency across the different test cases. Figure 11 (b) is a plot of Tensile Strength (MPa) against frequency along the y-axis for the experimentally measured tensile strength distribution. The data are very concentrated between 130 MPa and 150 MPa, indicating uniform mechanical behaviour among samples. Figure 11(c) plots Predicted Tensile Strength (MPa) vs. frequency on the y-axis. The spread is larger than that of the experimental data, from ~50 MPa to ~280 MPa. This indicates that the model exhibits greater variance and occasionally overestimates strength, possibly due to overfitting or the underrepresentation of outliers during training. Proceeding to elongation, Figure 11 (d) graphs Elongation (%) against the x-axis and frequency against the y-axis for experimental values. Most values fall within the expected ductility range of the tested composites, 3.0% to 5.0%. Figure 11 (e) indicates Predicted Elongation (%) on the x-axis and frequency on the y-axis. The distribution is highly similar to the experimental data but slightly less concentrated, indicating that the model

ARTICLE IN PRESS

satisfactorily captures elongation trends with reasonable accuracy. Figure 11(f) presents a further model-predicted elongation distribution with additional data bins, illustrating the model's ability to reproduce experimental behaviour in the 3.5–5.5% region. The residual plot begins with Figure 11(g), with the x-axis representing residuals (observed-predicted) in MPa and the y-axis representing frequency. The plot of the graph shows a moderate negative skew in the tensile-strength predictions, with residuals mostly ranging from -100 MPa to +50 MPa. This finding suggests that the model underestimates tensile strength, although there are sporadic cases of overestimation. Figure 11(h) displays residuals for elongation on the x-axis and frequency on the y-axis. The residuals are tightly between -2.5% and 0%, indicating very high accuracy and minimal overestimation of the elongation predictions. In conclusion, Figure 11(i) presents a scatter plot in which the x-axis represents the Predicted Tensile Strength (MPa), while the y-axis denotes the Predicted Elongation (%). The evident positive correlation depicted in this graph indicates that samples expected to have higher tensile strength are also likely to exhibit greater elongation, which aligns with empirical observations and supports the model's capacity to learn further. In short, although the model performs well in predicting elongation with a tight residual distribution, it is less variable in predicting tensile strength. Nonetheless, the predicted tensile-strength versus elongation relationship corresponds well with the experimental results, thereby improving the validity of the model for multi-property optimisation of Onyx fibre composites.

3.5. Performance Evaluation of Machine Learning Models for Flexural Strength Prediction

The interaction-based regression framework was proposed for the prediction of the flexural strength of the Onyx–Carbon Fibre composite material system. The modelling was based on the experimental data set created by the Taguchi L27 design of experiments, consisting of 162 experimental data samples with six replicates for every parameter configuration. Before the modelling, the experimental data samples for the same parameter configurations were combined for the preservation of the original configurations during the data splitting process. The experimental data samples for the proposed regression model were split based on the configurations by an 80:20 data splitting ratio, resulting in 126 experimental data samples for the regression modelling process and 36 data samples for the independent data verification process. This splitting was done such that no data samples for the same configurations were present in both the data splitting processes, thus avoiding any potential information overlap between the data samples.

To improve the stability of the regression learning process while staying within the validated experimental domain, data augmentation was applied under strict constraints for the experimental data samples, exclusively for

ARTICLE IN PRESS

the data samples intended for the regression modelling process, using the MATLAB programming environment. The data augmentation process was constrained by statistical considerations, staying strictly within the physically admissible domain as defined by the experimental data set. As a result, the data samples for the regression modelling process increased from 126 data samples to 447 data samples, while the data samples for the independent data verification process, consisting entirely of experimental data samples, was excluded from the optimization process and was kept constant at 36 data samples.

The regression model was implemented using the MATLAB programming environment by invoking the fitlm function, accounting for the interaction effects between the six governing parameters, namely, the material composition, the infill pattern, the infill density, the fibre volume fraction, the fibre orientation, and the roof floor layer count. Categorical variables have been defined using the categorical data type available in MATLAB, which has been internally represented by indicator variables, also known as one-hot encoding, during the regression fitting stage. The robustness of the regression model was determined by performing the cross-validation process on the regression model for five folds on the data samples intended for the regression modelling process. The performance of the interaction-based linear regression model was evaluated by implementing the 5-fold cross-validation technique to ensure the statistical robustness of the developed regression model, avoiding overfitting in the process. The interaction-based linear regression model was found to have an R^2 of 0.99, an RMSE of 5.24 MPa, a MAE of 4.07 MPa, and an MAPE of 5.3%. These findings indicate that the interaction-based linear regression model has an excellent correlation between the experimentally obtained results and the results obtained through the interaction-based linear regression model, as depicted in Table 9.

ARTICLE IN PRESS

Table 9. Performance Comparison of Top Five Regression Models

Model No.	Model Type	R^2 Score	RMSE (MPa)	MAE (MPa)	MAPE (%)	Remarks
2.2	Linear Regression	0.99	5.24	4.07	5.3	Top performer; SHAP shows Material Composition and Infill Pattern are most influential
3.1	Regression Tree	0.97	6.12	4.8	6.2	Interpretable structure; performs well with categorical inputs
4.3	Random Forest	0.98	5.5	4.1	5.5	Handles complex nonlinear relationships; stable predictions
5.4	SVM Regression	0.95	7	5.3	7.1	Accurate but computationally intensive
6.5	Boosted Trees	0.97	5.8	4.3	5.8	Good generalisation; ensemble-based strength.

ARTICLE IN PRESS

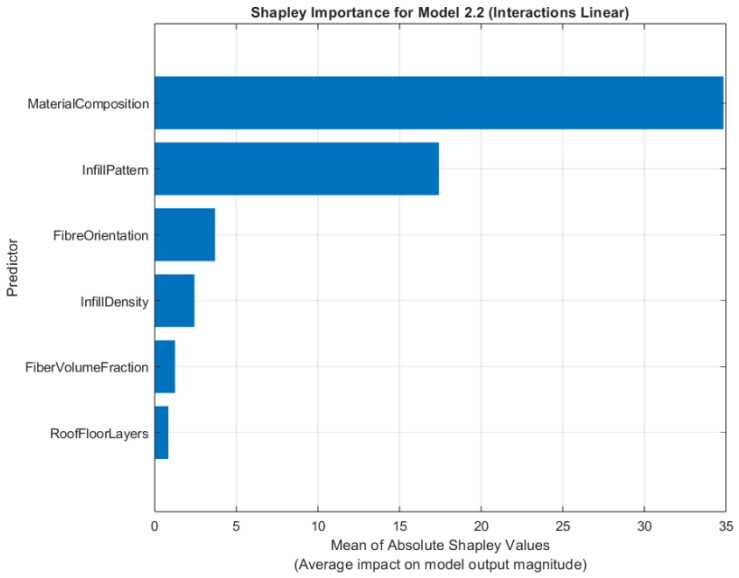

Figure 12. *SHAP Feature Importance Plot for Model 2.2 (Linear Regression)*

To gain a better understanding of the impact of each of the input parameters on Model 2.2 (Linear Regression) predictive performance, a SHAP (Shapley Additive Explanations) value analysis was conducted. The feature importance visualisation, as a result, estimates the mean absolute SHAP value for each predictor, thereby approximating its average contribution to the model's output. in this case, the predicted flexural strength. Among the predictors used, Material Composition has the most considerable SHAP value, indicating that it makes the greatest significant contribution to the determination of the flexural strength of the printed composite specimens. This is not surprising, since both the base material and the fibre reinforcement contribute directly to the composite's mechanical behaviour. The Infill Pattern was the second most important parameter, demonstrating the importance of internal geometry in defining the structural performance of the produced parts. Fibre Orientation and Infill Density both contributed moderately to the model, indicating that they influence load distribution and density-dependent material stiffness. In contrast, Fibre Volume Fraction and Roof Floor Layers demonstrated relatively low SHAP values, indicating a low individual contribution to the model output under the current dataset's conditions. These findings enable parameter ranking necessary for optimising flexural strength and provide a data-driven basis for experimental design and optimisation.

ARTICLE IN PRESS

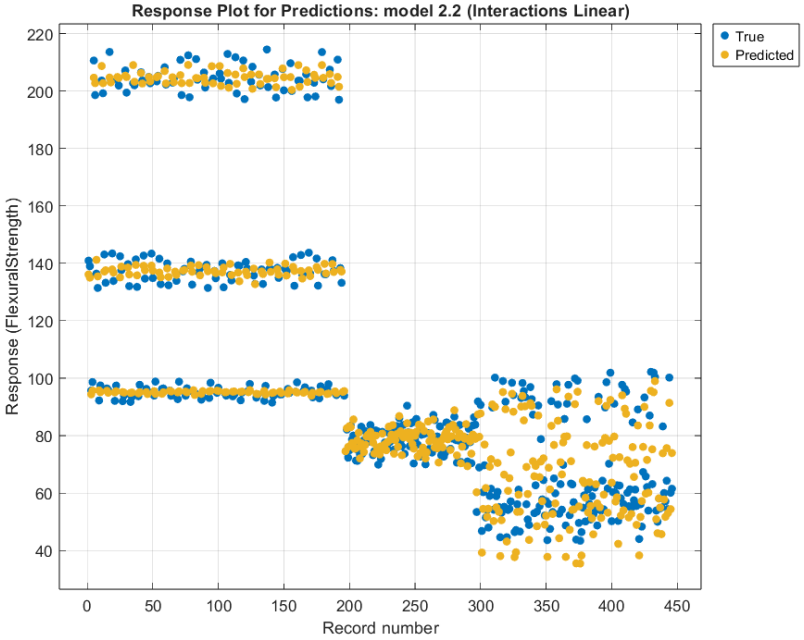

Figure 13. Response plot showing predicted versus actual values of flexural strength for Model 2.2 (Linear Regression).

The response plot in Figure 13 illustrates the quality of the model predictions by comparing predicted and actual flexural strengths for all samples in the dataset. Every point on the plot is a sample; blue points indicate the actual experimental values, and yellow points indicate the corresponding predicted values calculated by the linear regression model. There is a strong correlation between the predicted and measured responses across the entire data range. The data plot is a collection of horizontal clusters of data points, characteristic of different classes or levels of flexural strength, likely representing different batches of material or similar print conditions. Within each cluster, there is close agreement between the predicted responses and the measured values, indicating that the model provides a good representation of the underlying data relationships. The deviation between actual and predicted values is minimal, especially in regions of higher strength, approximately 200 MPa and 140 MPa, indicating excellent model performance for more rigid composites. However, there is somewhat greater variance in the weaker regions, especially those below 80 MPa, where the predictions deviate slightly from the actual values. This is due to higher noise, nonlinearity, or poorly modelled feature combinations in this specific range. Lastly, the graphical response plot is consistent with the quantitative measure statistics (e.g., $R^2 = 0.99$, RMSE = 5.24 MPa), confirming that Model 2.2 is highly accurate in forecasting flexural strength using the given process parameters. The graphical correlation between predicted and measured values confirms that the model has excellent generalisation capability across various input conditions.

ARTICLE IN PRESS

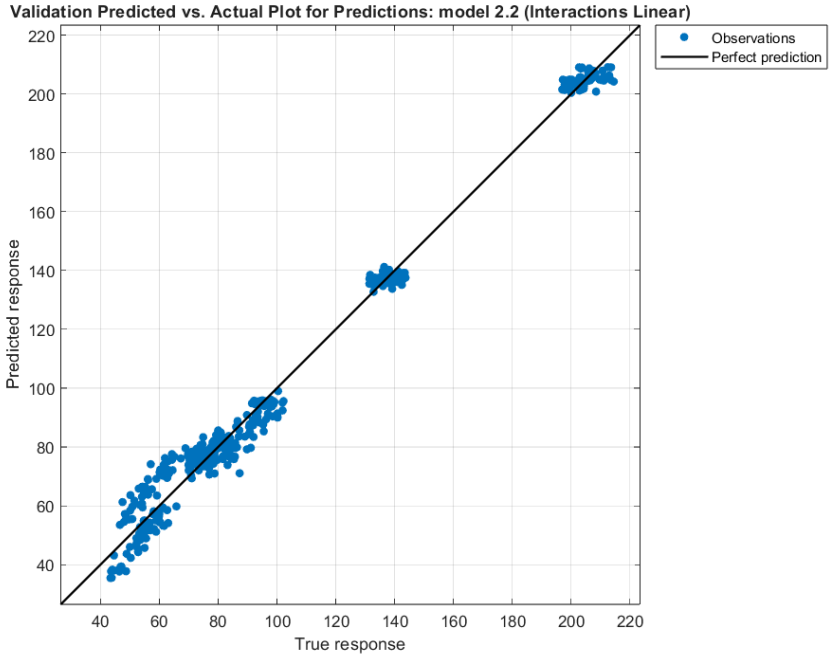

Figure 14. Predicted vs. actual flexural strength for Model 2.2 (Linear Regression).

Figure 14 shows the predicted and measured flexural strengths for Model 2.2 (Linear Regression). The points are very close to the 45° reference line, indicating that the predictions are highly accurate. The distribution is linear across the entire strength range (40–220 MPa), with no significant bias or scatter. This aligns with the model's high-performing metrics (R^2 = 0.99, RMSE = 5.24 MPa), indicating that it is precise and can be applied to other cases.

ARTICLE IN PRESS

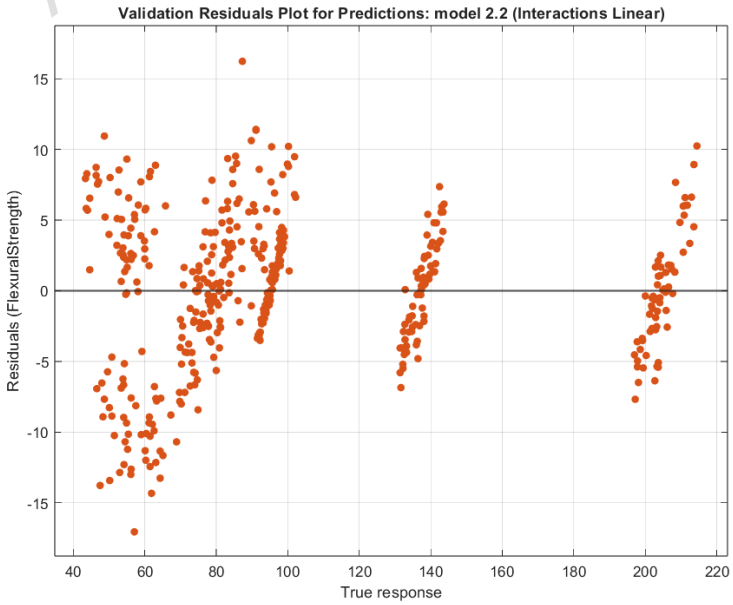

ARTICLE IN PRESS

Figure 15. Residual Analysis for Flexural Strength Predictions – Interaction Linear Model

Validation of the machine learning model (Model 2.2 – Linear Regression with interactions) was complemented by a strong set of graphical analyses. The response plot showed that the actual and predicted flexural strength values were extremely close across all samples, demonstrating high predictive accuracy. The scatter plot of predicted versus actual values showed a firm linear fit along the 45° line, again demonstrating the model's accuracy, consistent with its high R^2 value of 0.99. The residual plot also showed that the prediction errors were randomly scattered around zero, with no visible trend or variation, indicating that the model was well-behaved across all experimental conditions and unbiased. The SHAP feature importance analysis also showed that Material Composition and Infill Pattern were the most significant factors on the flexural strength. When we examined results from the multiple linear regression (MLR) model constructed in Section 3.4, we observed strong agreement in trend. The regression model yielded an R^2 of 99.94%, with highly significant coefficients for Onyx+CF, Gyroid pattern, and a 30% fibre volume fraction. The findings concurred with the machine learning model's SHAP-based rankings and values. Both models also concurred that fibre orientation (optimally 0°–30°) and infill density (~50%) enhance flexural performance, but the number of roof and floor layers had no influence. Both machine learning models and statistical regression models confirm each other, indicating that the selected input parameters are robust and significant. Both techniques provide a transparent and efficient way to forecast and enhance flexural strength in 3D-printed Onyx fibre-reinforced composites. The two-way methodology is helpful for process planning and material selection in additive manufacturing.

3.6. SEM Analysis of Failure Mechanisms in Onyx Fibre Composites

Figure 16 presents scanning electron microscope (SEM) images of the fractured surface of carbon fibre (CF) and glass fibre (GF)-reinforced Onyx-based composites subjected to tensile and flexural loading. The CF–Onyx specimens after the tensile test are presented in images (a) and (b), with microstructural characteristics of voids and microcracks marked. These voids represent poor interfacial bonding or insufficient fusion during additive manufacturing, acting as stress concentrators that lead to premature failure. The brittle fracture behaviour, as evidenced by microcrack development, is consistent with the reported high tensile strength and low elongation experimentally observed for CF composites, reflecting a stiff, abrupt failure mode. In Figure 17, Images (a) and (b) of GF–Onyx composites subjected to tensile loading similarly show voids, but to a lesser extent. The presence of crack growth patterns reflects a relatively ductile failure mode. This observation is consistent with the moderate tensile strength and greater elongation exhibited by GF–Onyx samples compared to CF–Onyx, reflecting the incorporation of glass fibre, which enhances compliance at the cost of reduced strength.

ARTICLE IN PRESS

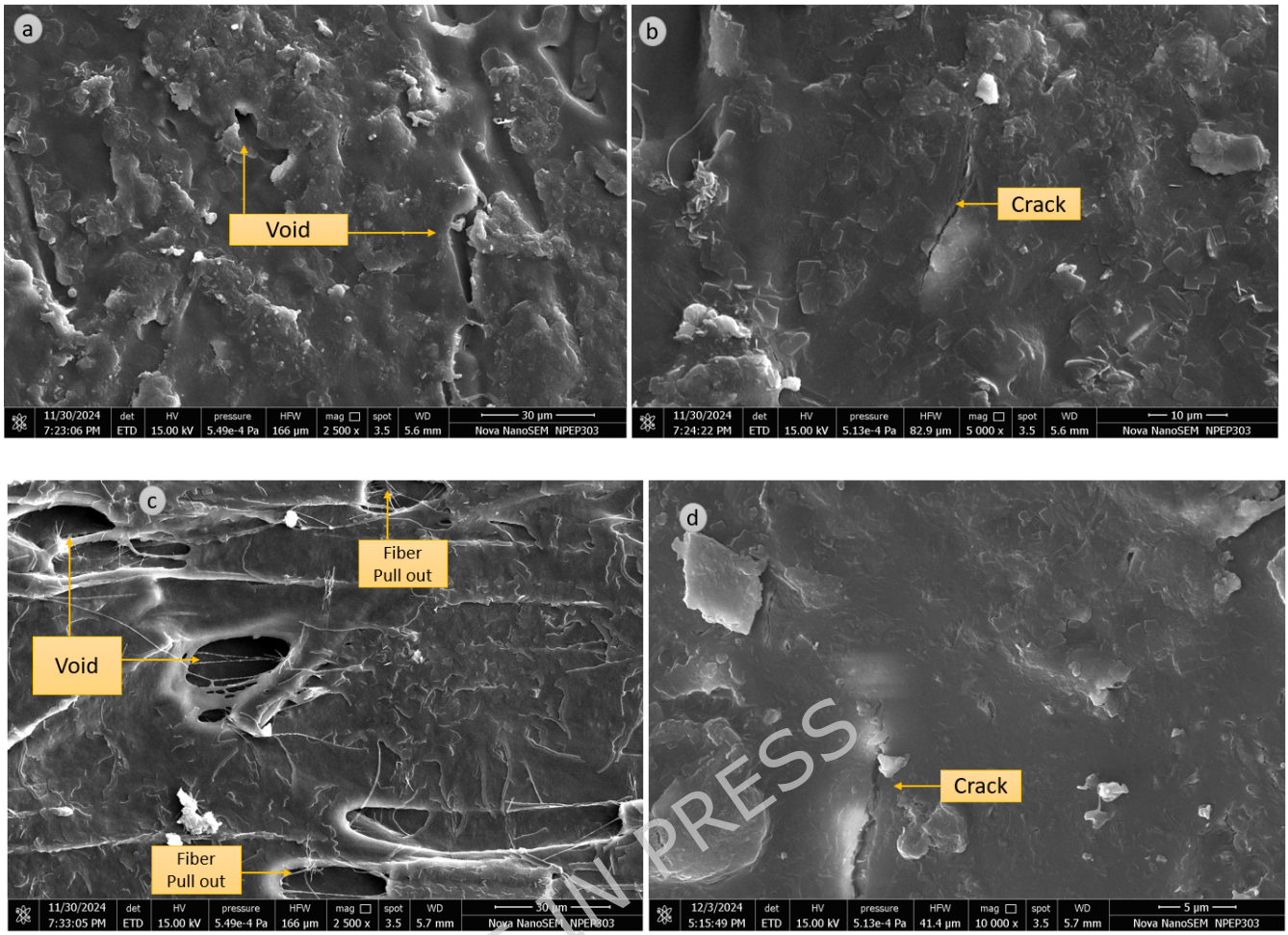

Figure 16. SEM microstructural analysis of Onyx-based fibre-reinforced composites:(a–b) CF–Onyx tensile fracture showing voids and cracks, (c–d) CF–Onyx flexural failure showing fibre pull-out and cracks

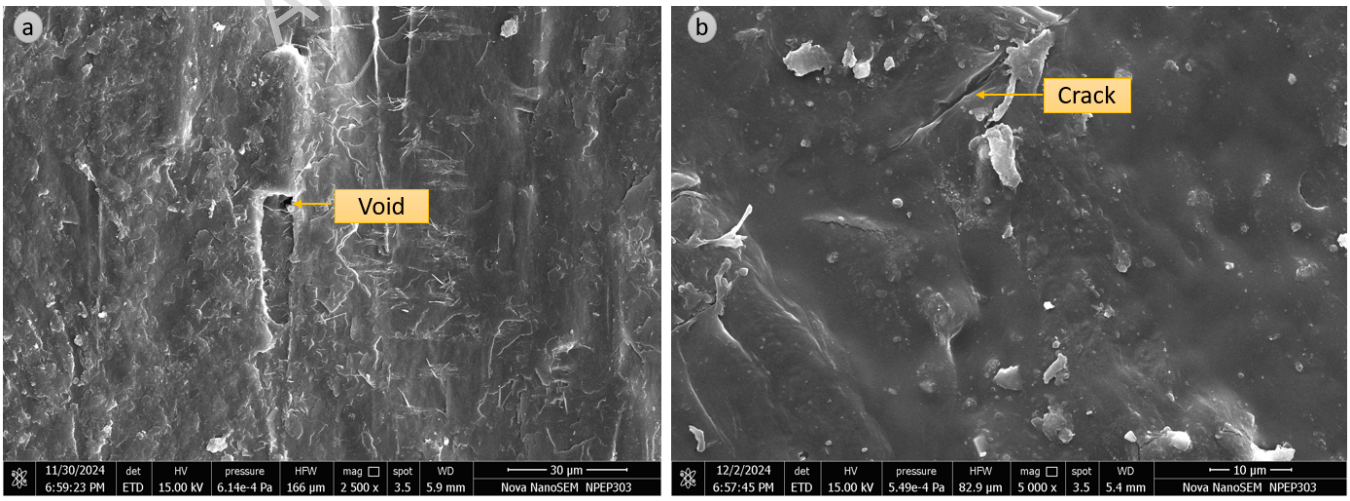

ARTICLE IN PRESS

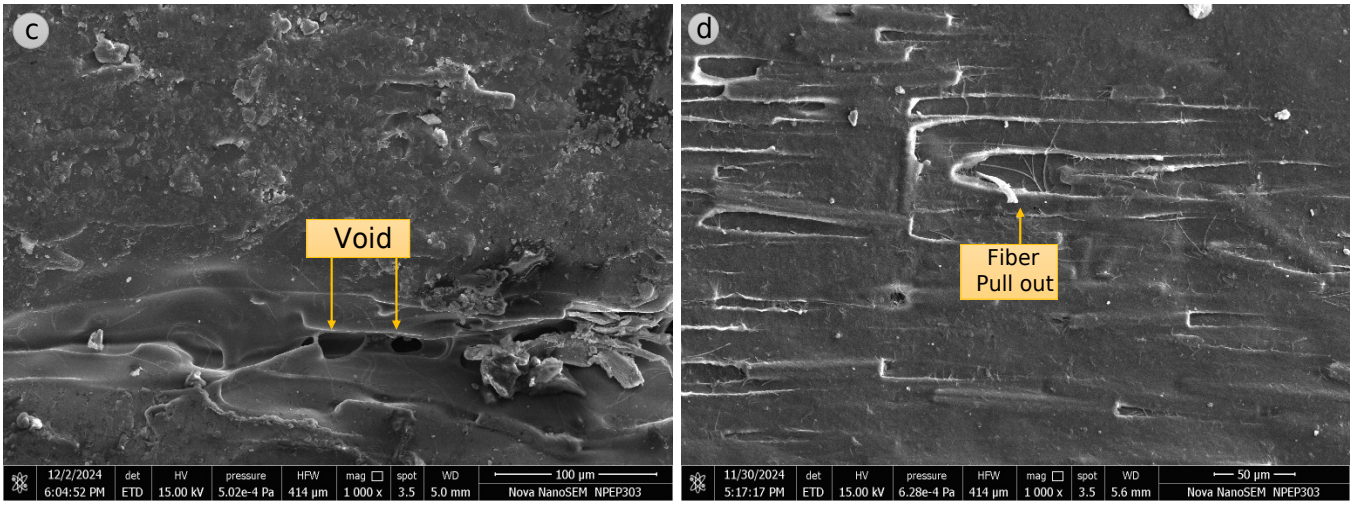

Figure 16. SEM microstructural analysis of Onyx-based fibre-reinforced composites:(a–b) GF–Onyx tensile fracture with voids and matrix cracks, (c–d) GF–Onyx flexural failure with voids and extensive fibre pull-out

ARTICLE IN PRESS

ARTICLE IN PRESS

In flexural loading conditions, Figure 16 images (c) and (d) show fracture surfaces of CF–Onyx composites containing voids and fibre pull-out. These show matrix–fibre debonding on the tensile side of the bend and contribute to energy absorption through fibre pull-out. However, the phenomenon is still dominated by brittle fracture owing to the low ductility of carbon fibres. However, Figure 17 images (c) and (d) of GF–Onyx flexural specimens show larger voids and larger fibre pull-out. Such structural features exhibit poor interfacial bonding, yet result in a more ductile response to flexural loading. The dominance of matrix cracking and large fibre pull-out is associated with the observed moderate flexural strength and increased strain-to-failure of GF-reinforced composites. The overall SEM analysis corroborates the mechanical test results, indicating that CF–Onyx composites exhibit brittle failure due to their high stiffness, whereas GF–Onyx composites exhibit more ductile failure modes, increasing deformability at the expense of strength.

3.7. Validation of Experimental Results with Published Literature

Table 11. Comparison of Present Experimental Results with Published Literature

Study	**Material System**	**Key Processing Parameters**	**Reported Tensile / Flexural Strength**	**Key Comparative Insight**
Present study	Onyx–CF / Onyx–GF	Taguchi L27, gyroid infill 52%, fibre vol. 30%, 0° orientation	CF tensile: 286.8 MPa; CF flexural: 206.4 MPa; GF flexural: 74.3 MPa	Reference dataset
Cofaru et al. (2022)	Onyx–CF	14 CF layers, 40% infill	Tensile: 290.6 MPa	Nearly identical CF tensile strength
Dantas et al. (2020)	Onyx–CF	12 CF layers, 0°/90°	Tensile: 278 ± 8 MPa	Same order, within experimental scatter
Lee et al. (2023)	Onyx–CF / GF	1–4 fibre layers, grid infill	CF tensile: ~200–300 MPa (converted)	The present CF result lies within the reported range
Ansari et al. (2022)	Onyx–CF / GF	Taguchi DOE, triangular 50%	CF flexural: 94.3 MPa; GF flexural: 65.7 MPa	Higher flexural due to gyroid infill
Yun et al. (2024)	Onyx–GF	1–4 GF layers, 100% infill	Tensile: 44.8–146 MPa	Lower strength; consistent GF trend
Zmindak et al. (2020)	Onyx–CF	0°/45°/90° orientation	Tensile: 188 MPa (0°)	Confirms the dominant role of 0° orientation

ARTICLE IN PRESS

The experimental results obtained in this study are in good agreement with those of previously published studies on Onyx-based continuous fibre composites prepared by fused filament fabrication. The experimental tensile strength of carbon fibre-reinforced Onyx specimens (286.8 MPa at 0° fibre orientation) is comparable to the values reported by Cofaru et al. (290.6 MPa) and Dantas et al. (278 ± 8 MPa), indicating high repeatability of the results among different studies, despite the differences in the infill pattern and number of fibre layers, as detailed in Table 11.

The flexural strength of CF-reinforced specimens (206.4 MPa) is higher than the values reported in Taguchi-based studies on specimens with triangular or rectilinear infill patterns, such as Ansari et al., in which the CF flexural strength was restricted to 94.3 MPa. This is because the gyroid infill pattern used in this study is more effective at enhancing load transfer and stress distribution.

The glass fibre-reinforced Onyx specimens showed lower tensile and flexural strength values but higher ductility, as reported by Yun et al. and Kumar et al. Among all the studies cited above, fibre orientation in the loading direction (0°) is the most prominent factor influencing tensile properties, thereby establishing the repeatability of the results.

The proposed framework was intended to ensure consistency and feasibility in the experiments. Some printing parameters, including nozzle size, raster width, and layer thickness, were thus kept constant to improve consistency and minimise process variability. Although this might reduce geometric variability, it allows for easy comparison of the important parameters that affect the mechanical properties of Onyx-based continuous fibre composites. The proposed models are therefore appropriate for the specific material-process combination and can be used as a basis for future expansion.

ARTICLE IN PRESS

4. Conclusion

This research work explains how fibre type, infill pattern, and fibre volume fraction interact to control the mechanical properties of 3D-printed Onyx composites. Carbon fibre-reinforced Onyx showed the highest tensile strength of 286.8 MPa and flexural strength of 206.4 MPa, due to the higher stiffness of the carbon fibres, which facilitates optimal load transfer and restricts matrix deformation, indicating a strength-controlling but brittle failure mode. Conversely, glass fibre-reinforced Onyx showed a relatively lower tensile strength of ~190 MPa but higher elongation of >4% due to reduced fibre-matrix bonding and increased fibre pull-out, which facilitates easy energy dissipation and ductility.

Analysis of variance revealed that the infill pattern ($F = 306.51$, $p < 0.001$) and fibre volume fraction ($F = 196.59$, $p < 0.001$) were the most dominant factors influencing tensile strength, as they directly control internal load paths, stress distributions, and fibre engagements within the 3D-printed

ARTICLE IN PRESS

structure. The best performance of the gyroid infill pattern with a 30% fibre volume fraction is due to its ability to support continuous stress transfer and reduce stress concentrations, which provide a highly predictive regression model (R^2 = 99.44%, Predicted R^2 = 96.75%).

These findings are supported by the machine learning results, which show that the Random Forest Regressor yields R^2 values of 0.94 for tensile strength and 0.89 for elongation. The high predictive consistency is attributed to ensemble learning's ability to better model nonlinear relationships among process variables than standalone models. These findings are further supported by scanning electron microscopy analysis, which shows that CF–Onyx composites exhibit microcracking and short-fibre pull-out, indicative of high strength and brittle failure, while GF–Onyx composites exhibit longer-fibre pull-out with voids, accounting for their increased toughness.

Taken together, the findings of this study demonstrate that the combination of structured experimentation and explainable machine learning is not only capable of making highly accurate predictions of mechanical properties but also provides explanatory power regarding the underlying reasons for the strength- or toughness-dominated failure modes of particular process-material combinations.

5. Future Scope

Further exploration of hybrid fibre combinations in Onyx to optimise strength and toughness balance, and Investigation of fatigue, impact, and thermal properties for high-performance structural applications.

6. Ethical Statements

This research is not founded on human subjects, animal experiments, or data gathered from social media sites. The study aims to optimise 3D printing parameters for Onyx-Fibre composites using experimental methods, machine learning, and SEM analysis, without considering any ethical implications related to the above categories. All experimental procedures and analyses were performed in accordance with the relevant scientific and institutional guidelines.

7. **Data Availability Statement:** All data generated or analysed during this study are included in this published article.

8. Conflict of Interest

The authors declare that they have no conflicts of interest related to this study.

9. Declaration

ARTICLE IN PRESS

The authors declare no conflicts of interest for this research and affirm they have no known competing financial interests or personal relationships that could have been assumed to influence the work in this manuscript. The research was supported under the Student Research Project scheme by Symbiosis International (Deemed University) (University Reference No.: Approval/2024/1419) with an approved grant of ₹1,50,000. The funding source had no involvement in study design, data collection, data analysis, data interpretation, or writing of the manuscript. Additionally, as no human subjects or personal data were involved, the Consent to Participate and Consent to Publish statements are not applicable.

Funding: The authors acknowledge King Saud University for funding this research through the Ongoing Research Funding program (ORF-2026-164). This Article Was Co-Funded by The European Union Under the Refresh – Research Excellence For Region Sustainability And High-Tech Industries Project Number Cz.10.03.01/00/22_003/0000048 Via The Operational Programme Just Transition And Has Been Done In Connection With Project Students Grant Competition Sp2024/087 „Specific Research Of Sustainable Manufacturing Technologies “Financed By The Ministry Of Education, Youth And Sports And Faculty Of Mechanical Engineering VŠB-TUO. Article Has Been Done in Connection with Project Students Grant Competition Sp2024/087 „Specific Research Of Sustainable Manufacturing Technologies “Financed By The Ministry Of Education, Youth And Sports And Faculty Of Mechanical Engineering VŠB-TUO.

References

1. Jost EW, Moore DG, Saldana C. Evolution of global and local deformation in additively manufactured octet truss lattice structures. Additive Manufacturing Letters. Elsevier Inc.; 2021;1. https://doi.org/10.1016/j.addlet.2021.100010

2. Medvedev AE, Lu S, Qian M, Brandt M. The effect of interfacial alloy formation on the mechanical properties of the additively manufactured Ti6Al4V/Ti1Al8V5Fe microstructurally graded material. Materials Science and Engineering: A. Elsevier Ltd; 2024;918. https://doi.org/10.1016/j.msea.2024.147484

3. Kumaresan R, Kulandaivel S, Samykano M, Keng NW, Sharuzi W, Harun W, et al. Additive Manufacturing: An Overview of Printing Technologies. Journal of Advanced Research in Applied Sciences and Engineering Technology Journal homepage [Internet]. 2026;59:245–60. https://doi.org/10.37934/araset.59.2.245260

4. Anh NT, Quynh NX, Tung TT. Study on Topology Optimization Design for Additive Manufacturing. Engineering, Technology and Applied Science Research. Dr D. Pylarinos; 2024;14:14437–41. https://doi.org/10.48084/etasr.7220

5. Rithika K, Sudha J. Additive Manufacturing of Fiber-Reinforced Composites—A Comprehensive Overview. Polym Adv Technol [Internet]. 2024;35:e70002. https://doi.org/https://doi.org/10.1002/pat.70002

6. Sathish K, Kumar SS, Magal RT, Selvaraj V, Narasimharaj V, Karthikeyan R, et al. A Comparative Study on Subtractive Manufacturing and Additive Manufacturing. Advances

ARTICLE IN PRESS

in Materials Science and Engineering. Hindawi Limited; 2022. https://doi.org/10.1155/2022/6892641

7. Galib G, Silva FJG, Pedroso AF V., Campilho RDSG, Lucas R, Sales-Contini R de CM. A Comprehensive Review of Additive Manufacturing Technologies for Composite Materials. Journal of Mechanical Engineering and Manufacturing. Scilight Press Pty Ltd; 2025;2. https://doi.org/10.53941/jmem.2025.100002

8. Shafighfard T, Cender TA, Demir E. Additive manufacturing of compliance optimized variable stiffness composites through short fiber alignment along curvilinear paths. Addit Manuf. Elsevier B.V.; 2021;37. https://doi.org/10.1016/j.addma.2020.101728

9. Chu Y, Fu X, Luo Y, Canning J, Wang J, Ren J, et al. Additive Manufacturing Fiber Preforms for Structured Silica Fibers with Bismuth and Erbium Dopants. Light: Advanced Manufacturing. Ji Hua Laboratory; 2022. p. 358–64. https://doi.org/10.37188/lam.2022.021

10. Yang M, Kowsari K, Myrie NO, Espinosa-Hoyos D, Jagielska A, Kim S, et al. Additive manufacturing of high aspect-ratio structures with self-focusing photopolymerization. Light: Advanced Manufacturing. Ji Hua Laboratory; 2022. p. 542–71. https://doi.org/10.37188/lam.2022.032

11. Widyatmoko RH, Mahardika M, Arifvianto B, Sugijopranoto A. The Optimization of Infill Pattern and FFF Printing Parameters for Improving Flexural Strength for Carbon Fiber Reinforced Nylon. 2025. p. 385–98. https://doi.org/10.2991/978-94-6463-772-4_34

12. Ahmadifar M, Benfriha K, Shirinbayan M, Fitoussi J, Tcharkhtchi A. Mechanical behavior of polymer-based composites using fused filament fabrication under monotonic and fatigue loadings. Polymers and Polymer Composites. SAGE Publications Ltd; 2022;30. https://doi.org/10.1177/09673911221082480

13. Hamzat AK, Murad MS, Adediran IA, Asmatulu E, Asmatulu R. Fiber-reinforced composites for aerospace, energy, and marine applications: an insight into failure mechanisms under chemical, thermal, oxidative, and mechanical load conditions. Adv. Compos. Hybrid Mater. Springer Science and Business Media B.V.; 2025. https://doi.org/10.1007/s42114-024-01192-y

14. Faidallah RF, Hanon MM, Szakál Z, Oldal I. Mechanical characterization of 3D-Printed carbon fiber-reinforced polymer composites and pure polymers: Tensile and compressive behavior analysis. International Review of Applied Sciences and Engineering. Akademiai Kiado ZRt.; 2025;16:22–31. https://doi.org/10.1556/1848.2024.00796

15. Ahmad MN, Ishak MR, Mohammad Taha M, Mustapha F, Leman Z, Anak Lukista DD, et al. Application of Taguchi Method to Optimize the Parameter of Fused Deposition Modeling (FDM) Using Oil Palm Fiber Reinforced Thermoplastic Composites. Polymers (Basel). MDPI; 2022;14. https://doi.org/10.3390/polym14112140

16. Garba UH, Wang T, Tian Y, Tian C. Enhancing optimization and reducing machining time of freeform shapes through modeling, simulation, and Taguchi design of experiments with artificial neural networks. International Journal on Interactive Design and Manufacturing (IJIDeM) [Internet]. 2025;19:2629–44. https://doi.org/10.1007/s12008-024-01872-5

17. Alhazmi W, Jazaa Y, Althahban S, Mousa S, Abu-Sinna A, Abd-Elhady A, et al. Mechanical and Tribological Behavior of Functionally Graded Unidirectional Glass Fiber-Reinforced Epoxy Composites. Polymers (Basel). MDPI; 2022;14. https://doi.org/10.3390/polym14102057

18. Georgantzinos SK, Papadopoulou E, Bakalis P. Prediction of Anisotropic Mechanical Behavior in Fused Deposition Modeling-Printed Polylactic Acid Structures with Straight-Line

ARTICLE IN PRESS

Microstructure Using Taguchi Design. J Mater Eng Perform [Internet]. 2025; https://doi.org/10.1007/s11665-025-12381-1

19. Ansari AA, Kamil M. Investigation of flexural properties in 3D printed continuous fiber-reinforced polymer composites. IOP Conf Ser Mater Sci Eng. IOP Publishing; 2022;1248:012070. https://doi.org/10.1088/1757-899x/1248/1/012070

20. Ismail R, Paras Utami D, Arid Irfai M, Jamari J, Bayuseno AP. Mechanical properties of Carbon-matrix composites for a blade runner's artificial leg. Cogent Eng. Cogent OA; 2021;8. https://doi.org/10.1080/23311916.2021.1923382

21. Islam MN, Baxevanakis KP, Silberschmidt V V. Mechanical characterisation of AM nylon-matrix carbon-fibre-reinforced composite in tension. Mater Today Proc. Elsevier Ltd; 2022. p. 50–4. https://doi.org/10.1016/j.matpr.2022.08.527

22. Breseghello L, Naboni R. Toolpath-based design for 3D concrete printing of carbon-efficient architectural structures. Addit Manuf. Elsevier B.V.; 2022;56. https://doi.org/10.1016/j.addma.2022.102872

23. El Essawi B, Abdallah S, Ali S, Nassir Abdo Mohammed A, Susantyoko RA, Pervaiz S. Optimization of infill density, fiber angle, carbon fiber layer position in 3D printed continuous carbon-fiber reinforced nylon composite. Results in Engineering. Elsevier B.V.; 2024;21. https://doi.org/10.1016/j.rineng.2024.101926

24. Ari A, Bayram A, Karahan M, Karagöz S. Comparison of the mechanical properties of chopped glass, carbon, and aramid fiber reinforced polypropylene. Polymers and Polymer Composites. SAGE Publications Ltd; 2022;30. https://doi.org/10.1177/09673911221098570

25. Solidxperts. Carbon Fiber 3D Printing with Markforged. Solidxperts [Internet]. [cited 2025 Dec 2]; https://www.solidxperts.com/en/blog/carbon-fiber-3d-printing-with-markforged/?utm_source=chatgpt.com. Accessed 2 Dec 2025

26. Yadav M, Komal UK, Tewari A. Analysis of Open-Hole Tensile Characteristics of Additively Manufactured Continuous Glass Fiber/Onyx Composites. Polym Compos [Internet]. n/a. https://doi.org/https://doi.org/10.1002/pc.70253

27. Singh TJ, Samanta S. Characterization of Kevlar Fiber and Its Composites: A Review. Mater Today Proc. Elsevier Ltd; 2015. p. 1381–7. https://doi.org/10.1016/j.matpr.2015.07.057

28. Atsani SI, Sing SL. Optimization of Glass-Powder-Reinforced Recycled High-Density Polyethylene (rHDPE) Filament for Additive Manufacturing: Transforming Bottle Caps into Sound-Absorbing Material. Polymers (Basel). Multidisciplinary Digital Publishing Institute (MDPI); 2024;16. https://doi.org/10.3390/polym16162324

29. Sultana MN, Sarker OS, Dhar NR. Parametric optimization and sensitivity analysis of the integrated Taguchi-CRITIC-EDAS method to enhance the surface quality and tensile test behavior of 3D printed PLA and ABS parts. Heliyon. Elsevier Ltd; 2025;11. https://doi.org/10.1016/j.heliyon.2024.e41289

30. Hashmi WA, Rehman A, Lathkar GS, Attar PR, Zubairuddin M. Investigating the Combined Effect of FDM 3D Printing Parameters on Tensile Behavior of ABS Plastic Using Taguchi Method. 2024;12:2024. https://doi.org/10.37591/JoPC

31. Lee GW, Kim TH, Yun JH, Kim NJ, Ahn KH, Kang MS. Strength of Onyx-based composite 3D printing materials according to fiber reinforcement. Front Mater. Frontiers Media S.A.; 2023;10. https://doi.org/10.3389/fmats.2023.1183816

ARTICLE IN PRESS

32. Hendito[1] M, Halim A, Siahan E. Physical Characterization of Onyx-Carbon Fiber Reinforced Material using Taguchi Method [Internet]. Int. J. Innov. Sci. Res. Technol. 2023. www.ijisrt.com3322

33. Hiralal Dhage B, Khedkar NK. Predictive machine learning and printing parameter optimization for enhanced impact performance of 3D-printed Onyx-Kevlar composites. Discov Mater. Discover; 2025;5. https://doi.org/10.1007/s43939-025-00307-6

34. Frankowski A, Sluder I, Tan KT. Characterizing the IZOD Impact Strength of a 3D Printed Reinforced Carbon Fiber Composite Material with Varying Layup Orientations. 2024 Regional Student Conferences [Internet]. https://doi.org/10.2514/6.2024-86171

35. Moreno-Núñez BA, Guerrero-Alvarado MA, Salgado-Castillo A, Treviño-Quintanilla CD, Cuan-Urquizo E, Sánchez-Santana U, et al. Build and raster orientation effects on CFRP onyx/aramid impact absorption. Composites Part C: Open Access. Elsevier B.V.; 2024;14. https://doi.org/10.1016/j.jcomc.2024.100485

36. Nargis RA, Jack DA. Fiber Orientation Quantification for Large Area Additively Manufactured Parts Using SEM Imaging. Polymers (Basel). Multidisciplinary Digital Publishing Institute (MDPI); 2023;15. https://doi.org/10.3390/polym15132871

37. Papa I, Silvestri AT, Ricciardi MR, Lopresto V, Squillace A. Effect of Fibre Orientation on Novel Continuous 3D-Printed Fibre-Reinforced Composites. 2021; https://doi.org/10.3390/polym

38. Kaushik V, Kurra S, Adusumalli R. Structure–property relationships in 3D-printed onyx-based composites reinforced with continuous fibers: role of temperature and fiber orientation. Composites Part C: Open Access. Elsevier B.V.; 2025;18. https://doi.org/10.1016/j.jcomc.2025.100649

39. Bouché GA, Akono A-T. Micromechanics-based estimates on the macroscopic fracture toughness of micro-particulate composites. Eng Fract Mech [Internet]. 2015;148:243–57. https://doi.org/https://doi.org/10.1016/j.engfracmech.2015.09.037

40. Khosravani MR, Soltani P, Reinicke T. Failure and fracture in adhesively bonded 3D-printed joints: An overview on the current trends. Eng Fail Anal [Internet]. 2023;153:107574. https://doi.org/https://doi.org/10.1016/j.engfailanal.2023.107574

41. Zhang H, Dickson AN, Sheng Y, McGrail T, Dowling DP, Wang C, et al. Failure analysis of 3D printed woven composite plates with holes under tensile and shear loading. Compos B Eng. Elsevier Ltd; 2020;186. https://doi.org/10.1016/j.compositesb.2020.107835

42. Rojek I, Kopowski J, Lewandowski J, Mikołajewski D. Use of Machine Learning to Improve Additive Manufacturing Processes. Applied Sciences (Switzerland). Multidisciplinary Digital Publishing Institute (MDPI); 2024;14. https://doi.org/10.3390/app14156730

43. Udu AG, Osa-Uwagboe N, Adeniran O, Aremi A, Ghalati MK, Dong H. A Machine Learning Approach to Characterise the Mechanical Properties [Internet]. https://ssrn.com/abstract=4515794

44. YI M, XUE M, CONG P, SONG Y, ZHANG H, WANG L, et al. Machine learning for predicting fatigue properties of additively manufactured materials. Chinese Journal of Aeronautics. Elsevier B.V.; 2024. p. 1–22. https://doi.org/10.1016/j.cja.2023.11.001

45. A Allen AE, Tkatchenko A. Machine learning of material properties: Predictive and interpretable multilinear models [Internet]. 2022. https://www.science.org

46. Akbari P, Zamani M, Mostafaei A. Machine learning prediction of mechanical properties in metal additive manufacturing. Addit Manuf. Elsevier B.V.; 2024;91. https://doi.org/10.1016/j.addma.2024.104320

ARTICLE IN PRESS

47. Chen H, Liu Y, Balabani S, Hirayama R, Huang J. Machine Learning in Predicting Printable Biomaterial Formulations for Direct Ink Writing. Research. American Association for the Advancement of Science (AAAS); 2023;6. https://doi.org/10.34133/research.0197

48. Goh GD, Sing SL, Yeong WY. A review on machine learning in 3D printing: applications, potential, and challenges. Artif Intell Rev. Springer Science and Business Media B.V.; 2021;54:63–94. https://doi.org/10.1007/s10462-020-09876-9

49. TA O. Application of Machine Learning Tools to Material Science: A Mini-Review. Physical Science & Biophysics Journal. Medwin Publishers; 2024;8:1–6. https://doi.org/10.23880/psbj-16000269

50. Prada Parra D, Ferreira GRB, Díaz JG, Gheorghe de Castro Ribeiro M, Braga AMB. Supervised Machine Learning Models for Mechanical Properties Prediction in Additively Manufactured Composites. Applied Sciences (Switzerland). Multidisciplinary Digital Publishing Institute (MDPI); 2024;14. https://doi.org/10.3390/app14167009

51. Ratnavel R, Viswanath S, Subramanian J, Selvaraj VK, Prahasam V, Siddharth S. Predicting the Optimal Input Parameters for the Desired Print Quality Using Machine Learning. Micromachines (Basel). MDPI; 2022;13. https://doi.org/10.3390/mi13122231

52. Li Q, Fu N, Omee SS, Hu J. MD-HIT: Machine learning for materials property prediction with dataset redundancy control. 2023; https://doi.org/10.1038/s41524-024-01426-z

53. Dave GS, Pandhare AP, Kulkarni AP, Khankal DV. Innovative data techniques for centrifugal pump optimization with machine learning and AI model. PLoS One. Public Library of Science; 2025;20. https://doi.org/10.1371/journal.pone.0325952

54. Zhou HR, Yang H, Li HQ, Ma YC, Yu S, Shi J, et al. Advancements in machine learning for material design and process optimization in the field of additive manufacturing. China Foundry. Springer Nature; 2024. p. 101–15. https://doi.org/10.1007/s41230-024-3145-3

55. Hamzat AK, Salman UT, Murad MS, Altay O, Bahceci E, Asmatulu E, et al. Development of robust machine learning models for predicting flexural strengths of fiber-reinforced polymeric composites. Hybrid Advances. Elsevier B.V.; 2025;8. https://doi.org/10.1016/j.hybadv.2025.100385

56. Alyami M, Khan M, Fawad M, Nawaz R, Hammad AWA, Najeh T, et al. Predictive modeling for compressive strength of 3D printed fiber-reinforced concrete using machine learning algorithms. Case Studies in Construction Materials. Elsevier Ltd; 2024;20. https://doi.org/10.1016/j.cscm.2023.e02728

57. Ali A, Riaz RD, Malik UJ, Abbas SB, Usman M, Shah MU, et al. Machine Learning-Based Predictive Model for Tensile and Flexural Strength of 3D-Printed Concrete. Materials. MDPI; 2023;16. https://doi.org/10.3390/ma16114149

58. Sangaletti S, Aranda MT, Távara L, García IG. Effect of stacking direction and raster angle on the fracture properties of Onyx 3D printed components: A mesoscale analysis. Theoretical and Applied Fracture Mechanics. Elsevier B.V.; 2024;129. https://doi.org/10.1016/j.tafmec.2023.104228

59. Nikiema D, Balland P, Sergent A. Study of 3D-printed onyx parts reinforced with continuous glass fibers: Focus on mechanical characterization, analytical prediction and numerical simulation. J Compos Mater [Internet]. 2024;58:1717–36. https://doi.org/10.1177/00219983241247913

60. Vedrtnam A, Ghabezi P, Gunwant D, Jiang Y, Sam-Daliri O, Harrison N, et al. Mechanical performance of 3D-printed continuous fibre Onyx composites for drone applications: An experimental and numerical analysis. Composites Part C: Open Access. Elsevier B.V.; 2023;12. https://doi.org/10.1016/j.jcomc.2023.100418

ARTICLE IN PRESS

61. Nikiema D, Sène NA, Balland P, Sergent A. Study of walls' influence on the mechanical properties of 3D printed onyx parts: Experimental, analytical and numerical investigations. Heliyon. Elsevier Ltd; 2023;9. https://doi.org/10.1016/j.heliyon.2023.e19187

62. Ma C, Faust J, Roy-Mayhew JD. Drivers of mechanical performance variance in 3D-printed fused filament fabrication parts: An Onyx FR case study. Polym Compos. John Wiley and Sons Inc; 2021;42:4786–94. https://doi.org/10.1002/pc.26187

63. Shafique N, Khan Z, Khan M, Younas M, Saharudin MS. Optimizing Process Parameters to Enhance Mechanical Properties of 3D-Printed Fiberglass-Reinforced ONYX Polymer. Journal of Manufacturing and Materials Processing. Multidisciplinary Digital Publishing Institute (MDPI); 2025;9. https://doi.org/10.3390/jmmp9040108

64. Ramalingam PS, Mayandi K, Balasubramanian V, Chandrasekar K, Stalany VM, Munaf AA. Effect of 3D printing process parameters on the impact strength of onyx – Glass fiber reinforced composites. Mater Today Proc. Elsevier Ltd; 2020. p. 6154–9. https://doi.org/10.1016/j.matpr.2020.10.467

65. Mohammed R, Badruddin IA, Shaik AS, Kamangar S, Khan AA. Experimental Investigation on Mechanical Characterization of Epoxy-E-Glass Fiber-Particulate Reinforced Hybrid Composites. ACS Omega. American Chemical Society; 2024;9:24761–73. https://doi.org/10.1021/acsomega.4c01365

66. Phunpeng V, Saensuriwong K, Kerdphol T, Uangpairoj P. The Flexural Strength Prediction of Carbon Fiber/Epoxy Composite Using Artificial Neural Network Approach. Materials. Multidisciplinary Digital Publishing Institute (MDPI); 2023;16. https://doi.org/10.3390/ma16155301

67. Turla P, Kumar SS, Reddy PH, Chandra Shekar K. Processing and Flexural Strength of Carbon Fiber and Glass Fiber Reinforced Epoxy-Matrix Hybrid Composite [Internet]. www.ijert.org

68. Mohankumar HR, Benal MGM, Pradeepkumar GS, Tambrallimath V, Ramaiah K, Khan TMY, et al. Effect of Short Glass Fiber Addition on Flexural and Impact Behavior of 3D Printed Polymer Composites. ACS Omega. American Chemical Society; 2023;8:9212–20. https://doi.org/10.1021/acsomega.2c07227

69. Turla P, Kumar SS, Reddy PH, Chandra Shekar K. Processing and Flexural Strength of Carbon Fiber and Glass Fiber Reinforced Epoxy-Matrix Hybrid Composite [Internet]. www.ijert.org

70. Marciniak D, Sykutera D, Czyżewski P. Analysis of mechanical properties and structure of samples filled with continuous glass fiber produced in composite filament fabrication technology. Bulletin of the Polish Academy of Sciences: Technical Sciences. Polska Akademia Nauk; 2024;72. https://doi.org/10.24425/bpasts.2024.148841

71. El Essawi B, Abdallah S, Ali S, Nassir Abdo Mohammed A, Susantyoko RA, Pervaiz S. Optimization of infill density, fiber angle, carbon fiber layer position in 3D printed continuous carbon-fiber reinforced nylon composite. Results in Engineering. Elsevier B.V.; 2024;21. https://doi.org/10.1016/j.rineng.2024.101926

72. Moreno-Núñez BA, Abarca-Vidal CG, Treviño-Quintanilla CD, Sánchez-Santana U, Cuan-Urquizo E, Uribe-Lam E. Experimental Analysis of Fiber Reinforcement Rings' Effect on Tensile and Flexural Properties of Onyx™–Kevlar® Composites Manufactured by Continuous Fiber Reinforcement. Polymers (Basel). MDPI; 2023;15. https://doi.org/10.3390/polym15051252

73. Shin SJ, Lee JH, Jadhav S, Kim DB. Material-Adaptive Anomaly Detection Using Property-Concatenated Transfer Learning in Wire Arc Additive Manufacturing. International Journal

ARTICLE IN PRESS

of Precision Engineering and Manufacturing. SpringerOpen; 2024;25:383–408. https://doi.org/10.1007/s12541-023-00924-2

74. Vedrtnam A, Ghabezi P, Gunwant D, Jiang Y, Sam-Daliri O, Harrison N, et al. Mechanical performance of 3D-printed continuous fibre Onyx composites for drone applications: An experimental and numerical analysis. Composites Part C: Open Access. Elsevier B.V.; 2023;12. https://doi.org/10.1016/j.jcomc.2023.100418

75. Li Z, Liu Y, Liang Z, Liu Y. The Influence of Fused Deposition Modeling Parameters on the Properties of PA6/PA66 Composite Specimens by the Taguchi Method and Analysis of Variance. 3D Print Addit Manuf. Mary Ann Liebert Inc.; 2024;11:E773–86. https://doi.org/10.1089/3dp.2022.0306

76. Megersa GK, Sitek W, Nowak AJ, Tomašić N. Investigation of the Influence of Fused Deposition Modeling 3D Printing Process Parameters on Tensile Properties of Polylactic Acid Parts Using the Taguchi Method. Materials. Multidisciplinary Digital Publishing Institute (MDPI); 2024;17. https://doi.org/10.3390/ma17235951

77. Chen DC, Zheng Q De, Chen CH. Optimization of Tensile Strength and Cost-Effectiveness of Polyethylene Terephthalate Glycol in Fused Deposition Modeling Using the Taguchi Method and Analysis of Variance. Polymers (Basel). Multidisciplinary Digital Publishing Institute (MDPI); 2024;16. https://doi.org/10.3390/polym16223133

78. Lucchese A, Carinci F. Everstick® and Ribbond® fiber reinforced composites: Scanning Electron Microscope (SEM) comparative analysis [Internet]. Article in European Journal of Inflammation. 2011. https://www.researchgate.net/publication/272085792

79. Antrim RF. Determination of Fiber Content in Long Fiber Reinforced Composites by Scanning Electron Microscopy and Image Analysis [Internet]. Scanning Microsc. 1988. https://digitalcommons.usu.edu/microscopyAvailableat:https://digitalcommons.usu.edu/microscopy/vol2/iss4/16

80. Kalagi Rajashekar Patil Pradeepa shetty Raviprasad Sujith kumar Vinod GR. Mechanical Properties and SEM Analysis of Flax/Sisal/Sic Nano Powder Reinforced Hybrid Composites ARTICLE HISTORY KEYWORDS Flax Sisal SiC nanopowder Scanning Electron Microscope (SEM). 2017; https://doi.org/10.jmsse/2348-8956/5-5.4

81. de Assis PV, da Silva RJ, Braga GG, Ancelloti Junior AC, Silveira ME, Panzera TH, et al. Mechanical and statistical analysis of hand-woven jute fibre composite laminates with bio-based and synthetic matrices. Compos Struct. Elsevier Ltd; 2025;358. https://doi.org/10.1016/j.compstruct.2025.118982

82. Čuchor D, Kopás P, Bronček J, Brumerčík F. Experimental Determination of the Mechanical Properties of Onyx Material. Materials Research Proceedings. Association of American Publishers; 2023. p. 6–13. https://doi.org/10.21741/9781644902691-2

83. Anbalagan A, Launchbury EJ, Kauffman M, Pazhani A, Anthony Xavior M. Investigation on CFRP 3D printing build parameters and their effect on topologically optimised complex models. Mater Today Proc. Elsevier Ltd; 2023; https://doi.org/10.1016/j.matpr.2023.04.352

84. Lee GW, Kim TH, Yun JH, Kim NJ, Ahn KH, Kang MS. Strength of Onyx-based composite 3D printing materials according to fiber reinforcement. Front Mater. Frontiers Media S.A.; 2023;10. https://doi.org/10.3389/fmats.2023.1183816

85. Rodríguez JGD, Comas ADP, Herrera JDS. Notch sensitivity study in u-notched polymers built by Additive Manufacturing (AM). Frattura ed Integrita Strutturale. Gruppo Italiano Frattura; 2023;17:127–39. https://doi.org/10.3221/IGF-ESIS.66.07

86. Dantas F, Couling K, Gibbons GJ. Long-fibre reinforced polymer composites by 3D printing: influence of nature of reinforcement and processing parameters on mechanical

ARTICLE IN PRESS

performance. Functional Composite Materials. Springer Science and Business Media LLC; 2020;1. https://doi.org/10.1186/s42252-020-00010-0

87. Batu T, Lemu HG, Shimels H. Application of Artificial Intelligence for Surface Roughness Prediction of Additively Manufactured Components. Materials. Multidisciplinary Digital Publishing Institute (MDPI); 2023. https://doi.org/10.3390/ma16186266

88. Ghebretinsae F, Mikkelsen O, Akessa AD. Strength analysis of 3D printed carbon fibre reinforced thermoplastic using experimental and numerical methods. IOP Conf Ser Mater Sci Eng. IOP Publishing Ltd; 2019. https://doi.org/10.1088/1757-899X/700/1/012024

89. Žmindák M, Novák P, Soukup J, Milosavljevic D, Kaco M. Finite element simulation of tensile test of composite materials manufactured by 3D printing. IOP Conf Ser Mater Sci Eng. Institute of Physics Publishing; 2020. https://doi.org/10.1088/1757-899X/776/1/012082

90. Hyun GW, Yuk JC, Park SH. Mechanical Characterization of 3D Printed Fiber-Reinforced Composite Structures for Reinforcement Learning-Aided Design. International Journal of Precision Engineering and Manufacturing [Internet]. 2025; https://doi.org/10.1007/s12541-025-01235-4

91. Bárnik F, Vaško M, Sága M, Handrik M, Sapietová A. Mechanical properties of structures produced by 3D printing from composite materials. MATEC Web of Conferences. EDP Sciences; 2019;254:01018. https://doi.org/10.1051/matecconf/201925401018

92. Cofaru NF, Pascu A, Oleksik M, Petruse R. Tensile Properties of 3D-printed Continuous-Fiber-Reinforced Plastics. Materiale Plastice. Syscom 18 SRL; 2021;58:271–82. https://doi.org/10.37358/MP.21.4.5552

93. Jatti VS, Sapre MS, Jatti A V., Khedkar NK, Jatti VS. Mechanical Properties of 3D-Printed Components Using Fused Deposition Modeling: Optimization Using the Desirability Approach and Machine Learning Regressor. Applied System Innovation. MDPI; 2022;5. https://doi.org/10.3390/asi5060112

94. Hassan M, Misra M, Taylor GW, Mohanty AK. A review of AI for optimization of 3D printing of sustainable polymers and composites. Composites Part C: Open Access. Elsevier B.V.; 2024. https://doi.org/10.1016/j.jcomc.2024.100513

95. Karabulut M. Machine Learning-Driven Flexural Performance Prediction and Experimental Investigation of Glass Fiber-Reinforced Polymer Bar-Reinforced Concrete Beams. Polymers (Basel). Multidisciplinary Digital Publishing Institute (MDPI); 2025;17. https://doi.org/10.3390/polym17060713

96. Qian Y, Sufian M, Hakamy A, Farouk Deifalla A, El-said A. Application of machine learning algorithms to evaluate the influence of various parameters on the flexural strength of ultra-high-performance concrete. Front Mater. Frontiers Media S.A.; 2023;9. https://doi.org/10.3389/fmats.2022.1114510

97. Deshmankar AP, Challa JS, Singh AR, Regalla SP. A Review of the Applications of Machine Learning for Prediction and Analysis of Mechanical Properties and Microstructures in Additive Manufacturing. J. Comput. Inf. Sci. Eng. American Society of Mechanical Engineers (ASME); 2024. https://doi.org/10.1115/1.4066575

98. Eren Z, Burnett CA, Wright D, Kazancı Z. Compressive characterisation of 3D printed composite materials using continuous fibre fabrication. International Journal of Lightweight Materials and Manufacture. KeAi Publishing Communications Ltd.; 2023;6:494–507. https://doi.org/10.1016/j.ijlmm.2023.05.002

ARTICLE IN PRESS

99. Zhang J, Wang P, Gao RX. Deep learning-based tensile strength prediction in fused deposition modeling. Comput Ind. Elsevier B.V.; 2019;107:11–21. https://doi.org/10.1016/j.compind.2019.01.011

100. Alafaghani A, Qattawi A. Investigating the effect of fused deposition modeling processing parameters using Taguchi design of experiment method. J Manuf Process. Elsevier Ltd; 2018;36:164–74. https://doi.org/10.1016/j.jmapro.2018.09.025

ARTICLE IN PRESS